iScience

CellPress
OPEN ACCESS

Article

High resistance to *Toxoplasma gondii* infection in inducible nitric oxide synthase knockout rats

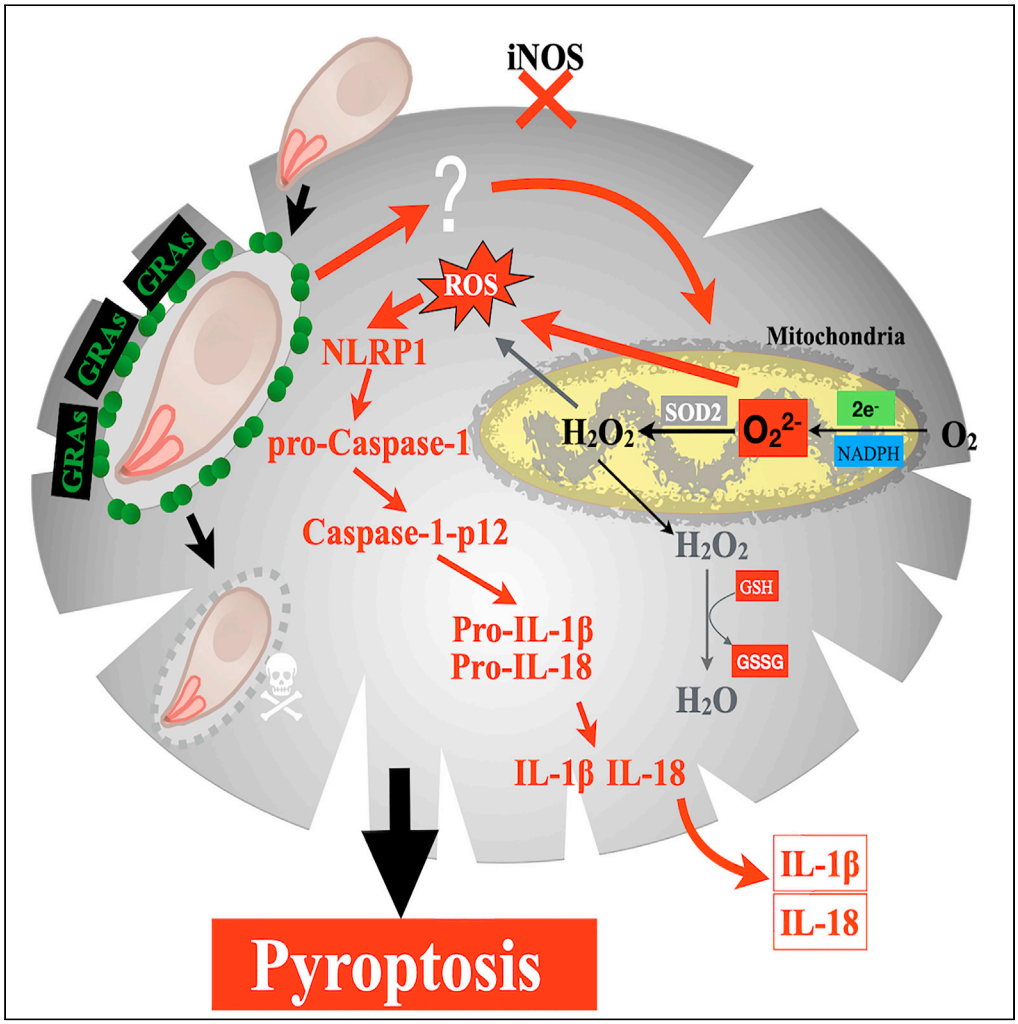

Zhen-Jie Wang, Shao-Meng Yu, Jiang-Mei Gao, ..., Masahiro Yamamoto, De-Hua Lai, Zhao-Rong Lun

lsslzr@mail.sysu.edu.cn (Z.-R.L.)
laidehua@mail.sysu.edu.cn (D.-H.L.)

Highlights

iNOS$^{-/-}$-SD rats show strong resistance to *Toxoplasma gondii* infection

iNOS$^{-/-}$-SD rat PMs resist *T. gondii* infection through ROS upregulation

The *T. gondii* infection results in PM pyroptosis in *iNOS*$^{-/-}$-SD rats

GRAs play a key role in the activation of resistance in *iNOS*$^{-/-}$-SD rat PMs

Wang et al., iScience 24, 103280
November 19, 2021
https://doi.org/10.1016/j.isci.2021.103280

iScience

CellPress
OPEN ACCESS

Article

High resistance to *Toxoplasma gondii* infection in inducible nitric oxide synthase knockout rats

Zhen-Jie Wang,[1] Shao-Meng Yu,[1] Jiang-Mei Gao,[2] Peng Zhang,[1] Geoff Hide,[3] Masahiro Yamamoto,[4] De-Hua Lai,[1,*] and Zhao-Rong Lun[1,2,3,5,*]

SUMMARY

Nitric oxide (NO) is an important immune molecule that acts against extracellular and intracellular pathogens in most hosts. However, after the knockout of inducible nitric oxide synthase (*iNOS*$^{-/-}$) in Sprague Dawley (SD) rats, these *iNOS*$^{-/-}$ rats were found to be completely resistant to *Toxoplasma gondii* infection. Once the *iNOS*$^{-/-}$ rat peritoneal macrophages (PMs) were infected with *T. gondii*, they produced high levels of reactive oxygen species (ROS) triggered by GRA43 secreted by *T. gondii*, which damaged the parasitophorous vacuole membrane and PM mitochondrial membranes within a few hours post-infection. Further evidence indicated that the high levels of ROS caused mitochondrial superoxide dismutase 2 depletion and induced PM pyroptosis and cell death. This discovery of complete resistance to *T. gondii* infection, in the *iNOS*$^{-/-}$-SD rat, demonstrates a strong link between NO and ROS in immunity to *T. gondii* infection and showcases a potentially novel and effective backup innate immunity system.

INTRODUCTION

Toxoplasma gondii is a globally distributed obligatory intracellular protozoan parasite that can infect a large number of warm-blooded vertebrates, including humans. It was estimated that one-third of the world's human population is infected with *T. gondii* (Dubey and Frenkel, 1998). Once infected, this opportunistic pathogen is able to invade and propagate in virtually all nucleated host cells of warm-blooded animals with the exception of birds' red blood cells (Dubey and Frenkel, 1998; Werk, 1985). Although chronic asymptomatic infection is found in most cases, it can cause severe toxoplasmosis in immunocompromised individuals including those who are undergoing chemotherapy, such as patients with AIDS, patients with cancer, and organ transplantation patients. It also causes abortion both in humans and domestic animals (Dupont et al., 2012; Flegr et al., 2014). It has long been known that there are huge differences in the outcome among different hosts infected with *T. gondii*, and the mechanisms of susceptibility and resistance are still hot topics to be investigated.

The mechanisms of host or host cell resistance to *T. gondii* infection have been extensively analyzed in mouse models. In these models, the resistance to *T. gondii* infection relies on a potent Th1 axis driven by IL-12-induced IFN-γ production (Dupont et al., 2012; Gazzinelli et al., 2014). This cytokine primes innate immune cells to express proinflammatory mediators, which favor the development of Th1 immune response against pathogens (James, 1995). In addition, the IFN-γ also uplifts the activity of inducible nitric oxide synthase (iNOS), which produces large amounts of nitric oxide (NO), a critical effector molecule that can restrict *T. gondii* growth in mice (Hunter and Sibley, 2012). NO is an essential signaling molecule in animals and is produced by a family of nitric oxide synthases (NOSs), including neuronal NOS (nNOS or NOS1), endothelial NOS (eNOS or NOS3), and particularly by inducible NOS (iNOS or NOS2), through the catalysis of L-arginine, the substrate of these enzymes (Alderton et al., 2001; Griffith and Stuehr, 1995; Martens et al., 2005; Masters et al., 1996; Nathan and Xie, 1994). NO, mainly produced by iNOS, is a primary killing factor of intracellular pathogens and plays an important role in the activity of macrophages (Bogdan, 2001; Schlüter et al., 1999). A large number of studies have demonstrated that NO is a microbiocidal substance and is cytotoxic against many pathogens including viruses, bacteria, fungi, protozoan, and helminth parasites (Chen, 2016; Croen, 1993; Karupiah et al., 1993; Nathan and Hibbs, 1991; Shen et al., 2017a, b). The importance of NO in the mouse has been discussed extensively for many decades. For example, following the knockout of the *iNOS* gene, mice were found to be more susceptible to the

[1]Guangdong Provincial Key Laboratory of Aquatic Economic Animals, State Key Laboratory of Biocontrol, School of Life Sciences, Sun Yat-Sen University, Guangzhou 510275, The People's Republic of China

[2]Department of Parasitology, Key Laboratory of Tropical Disease Control of the Ministry of Education, Zhongshan School of Medicine, Sun Yat-Sen University, Guangzhou 510080, The People's Republic of China

[3]Biomedical Research Centre, School of Science, Engineering and Environment, University of Salford, Salford M5 4WT, UK

[4]Department of Immunoparasitology, Research Institute for Microbial Diseases, Osaka University, Osaka, Japan

[5]Lead contact

*Correspondence: lsslzr@mail.sysu.edu.cn (Z.-R.L.), laidehua@mail.sysu.edu.cn (D.-H.L.)

https://doi.org/10.1016/j.isci.2021.103280

intracellular pathogens, *Leishmania, T. gondii,* and many others (Behnke et al., 2016; Croen, 1993; Yarovinsky, 2014).

The rat is another animal model system that has drawn recent attention in disease studies, particularly in the field of toxoplasmosis (Freyre et al., 2003a). Rats are highly resistant to *T. gondii* infection in comparison with mice, although the survival rate and tissue cyst numbers vary greatly among different rat strains and *T. gondii* strains (Freyre et al., 2003a, 2003b, 2004; Gao et al., 2015; Zenner et al., 1993). For example, when adults rats were orally infected with 200 *T. gondii* Prugniaud cysts, the Fischer 344 rat strain developed a large cyst burden (1231 ± 165.6, ranging from 820 to 1800), whereas four other strains of rat, including Brown Norway (BN), Sprague Dawley (SD), Wistar, and Lewis (LEW), developed no cysts (Gao et al., 2015). The subclinical pathology of toxoplasmosis in rats is similar to that found in humans, which may make it a better model for human toxoplasmosis than mice (Dubey and Frenkel, 1998). Many studies have demonstrated that NO might play an important role in the control of *T. gondii* infection in rats, and mechanisms for this resistance have been proposed (Cavailles et al., 2014; Gao et al., 2015; Witola et al., 2017). Specifically, the higher expression levels of iNOS in rats, compared with the lower expression of this gene found in mice, which are more susceptible, correlates with a greater resistance to *T. gondii* infection in rats (Li et al., 2012; Zhao et al., 2013). However, these studies only provided indirect evidence of the role of NO owing to the limitations of the genetic tools available in rats until recently. Recently, *iNOS* knockout ($iNOS^{-/-}$) SD rats were generated and used, in our laboratory, to directly reveal the role of NO against *Leishmania* and *Schistosoma* infections (Chen, 2016; Shen et al., 2017a, b). As NO plays different roles in mice and humans, we wished to understand the role of NO (or iNOS) in innate immunity against *T. gondii* infection in rats.

By using the $iNOS^{-/-}$-SD rat, we measured the resistance of this animal to *T. gondii* infection. Surprisingly, both results from in vitro and in vivo studies clearly demonstrated that the individuals and the macrophages from the $iNOS^{-/-}$-SD rats were completely resistant to the parasite infection. These results are unexpected and are contradictory to the results found for the mice model and may indicate a potential new or backup innate immunity system to control infections in rats.

RESULTS

$iNOS^{-/-}$-SD rats are resistant to *Toxoplasma gondii* infection

In earlier stages of this work, we thought that after the deletion of the *iNOS* gene the rat would become more susceptible to infection by *T. gondii* and other intracellular pathogens in a similar manner to that found in mice and for other parasites. Our results showed that about 40% wild-type (WT)-SD rats died within two weeks from infection with the *T. gondii* strains RH or Tgctsd1 (a virulent *T. gondii* strain isolated from a cat in Shandong Province, China) (Figure 1A). However, to our surprise, $iNOS^{-/-}$-SD rats did not display susceptibility but showed resistance to the infection when using different strains of *T. gondii* (Figure 1B), suggesting a significant burst of resistance after the knockout of *iNOS*. A brain cyst count in surviving rats revealed a relatively high burden in all examined WT-SD rats infected with strain Tgctsd1, but a lack of cysts in the 6 examined $iNOS^{-/-}$-SD rats (Figure 1C). A similar phenomenon was observed in infections with the *T. gondii* Prugniaud (Pru) strain, although a lower cyst burden was found.

To further confirm the resistance in $iNOS^{-/-}$-SD rats against *T. gondii* infection, homogenized brains and other organs from infected $iNOS^{-/-}$ and WT-SD rats were intraperitoneally (i.p.) injected into mice. None of the organ samples collected from the $iNOS^{-/-}$-SD rats were found to be positive after 10 days of infection with the *T. gondii* RH strain, while 17 brains, 2 spleens, and 13 lungs were found to be positive in the WT-SD groups (Table 1). This demonstrated that *T. gondii* could not survive in the $iNOS^{-/-}$-SD rats beyond, at least, 10 days post-infection (dpi). Similar results were obtained, on day 60, in the infection with other strains of *T. gondii*, PLK/RED, and Tgctsd1 (Table 1). In addition, the amount of IFN-γ in sera collected from both the $iNOS^{-/-}$ and WT-SD rats, 3–6 days after infection with *T. gondii*, was significantly increased (Figure S1).

To clarify the involvement of cells in the resistance to *T. gondii* in $iNOS^{-/-}$-SD rats, rat neonatal muscle fibroblast cells (NMFCs) were first tested. Both the WT and $iNOS^{-/-}$-SD rats' NMFCs were significantly resistant to the *T. gondii* RH/GFP strain when IFN-γ was supplemented in the medium (Figures 1E–1G). In addition, lipopolysaccharide (LPS) was also found to slightly enhance the resistance, and a synergistic effect was observed with IFN-γ. Similarities in the mode of resistance were observed when the *T. gondii*

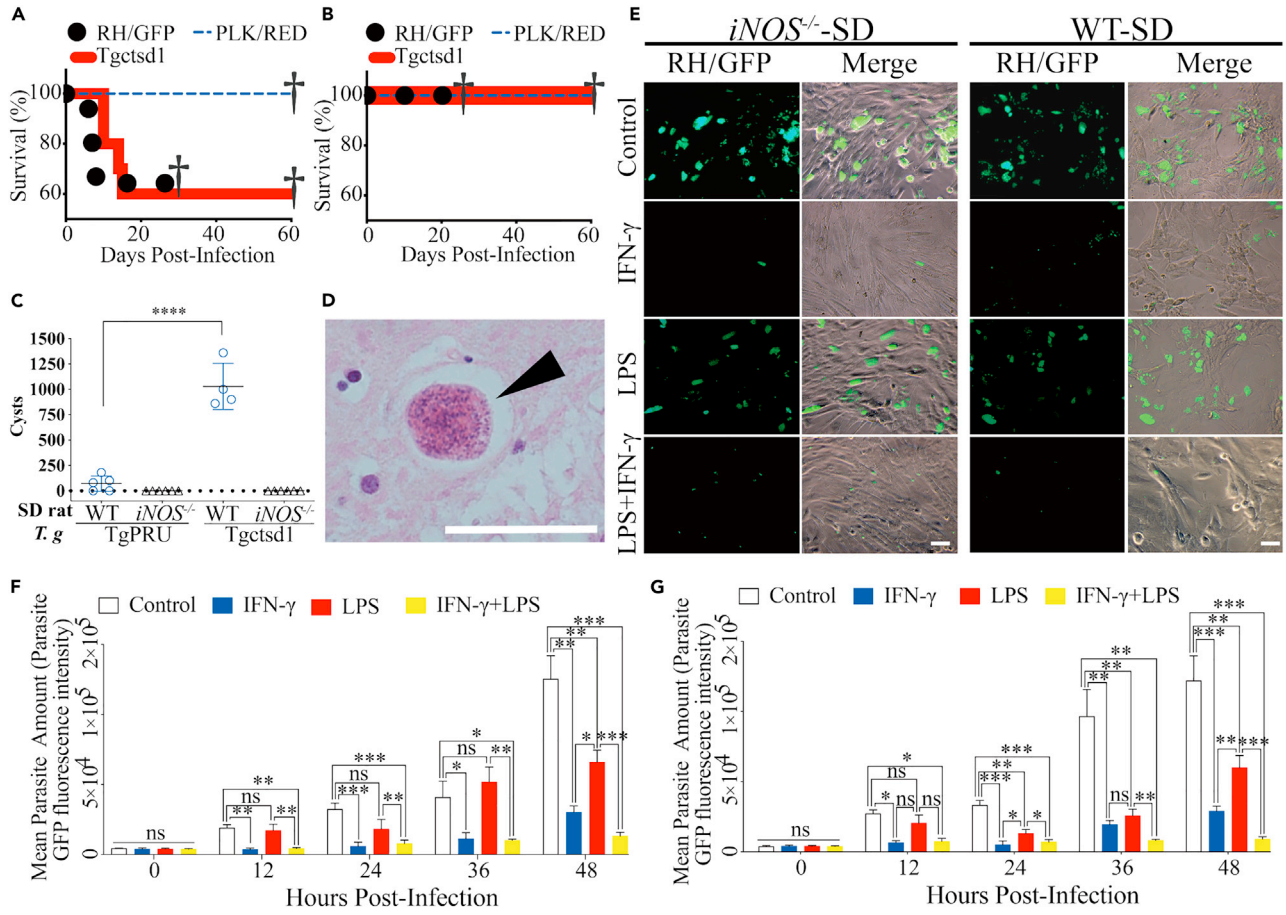

Figure 1. The *iNOS*$^{-/-}$-SD rat is completely resistant to *T. gondii*, and this is not dependent on muscle fibroblast cells

(A and B) The survival rate of WT-SD (A) and *iNOS*$^{-/-}$-SD (B) rats infected with three different strains of *T. gondii* (RH/GFP, PLK/RED, and Tgctsd1). Rats aged 4–5 weeks were intraperitoneally (i.p.) infected with 10^7 tachyzoites. Those infected with the non-cyst-forming strain, RH/GFP, were sacrificed at 30 days post-infection (dpi), and the rats infected with cyst-forming strains, PLK/RED or Tgctsd1, were sacrificed at 60 dpi to measure tissue cyst formation. A total of 9–14 rats per group were used.

(C) Brain cyst burdens in the rats infected with *T. gondii* Tgctsd1 (WT-SD, n = 5; *iNOS*$^{-/-}$-SD, n = 6) (a strain that has high cyst-forming capacity) and the Prugniaud (PRU) strain (WT-SD, n = 6; *iNOS*$^{-/-}$-SD, n = 6) (as a reference with moderate cyst-forming capacity). Rats, aged 4–5 weeks, were i.p. infected with 1×10^6 tachyzoites of *T. gondii* Tgctsd1 and Prugniaud (PRU) strains.

(D) A brain cyst was detected in brain tissue sections from a WT SD rat infected with *T. gondii* Tgctsd1 and stained with H&E (arrow), scale bar = 50 μm.

(E) *iNOS*$^{-/-}$-SD and WT-SD rat neonatal muscle fibroblast cells (NMFs) were infected with *T. gondii* RH/GFP strain tachyzoites in the medium with IFN-γ and LPS in 48 hpi, scale bars = 50 μm.

(F and G) The mean parasite loads, judged by fluorescence intensity, in *iNOS*$^{-/-}$-SD (F) and WT-SD (G) rat NMFs with or without IFN-γ and LPS. MOI = 2, cells were transferred into 24-well plates for further investigation; 5×10^5 per well; in triplicate; n = 3; all data are presented as mean ± SD and are representative of three independent experiments. *, $p < 0.05$; **, $p < 0.01$; ***, $p < 0.001$; ns, no significant difference. See also Figures S1 and S3.

PLK/RED strain was used (Figures S3A–S3C). The behaviors of rat NMFCs, with respect to resistance to *T. gondii* infection, were almost identical in both *iNOS*$^{-/-}$ and WT-SD rats. This suggested that the specific resistance in *iNOS*$^{-/-}$-SD rats against *T. gondii* infection might be independent of muscle cells.

iNOS$^{-/-}$-SD rat PMs showed strong resistance to *T. gondii* tachyzoite infection

After excluding the possibility that muscle fibroblasts were playing a major role in defense against *T. gondii*, we then asked the question of how *T. gondii* could be completely killed in the *iNOS*$^{-/-}$-SD rats? To our knowledge, this might not be a traditional immunological pathway that has previously been described that could account for this. It is well known that macrophages are primarily and frequently attacked by *T. gondii* and many other pathogens. We, therefore, focused on macrophages. Our results demonstrated that, although NO was not detected in the freshly obtained *iNOS*$^{-/-}$-SD rat PMs (Figure S2),

Table 1. Bioassay of organs from WT and *iNOS*$^{-/-}$-SD rats infected with different strains of *T. gondii* tachyzoites

	Blood		Brain		Heart		Liver		Spleen		Lung		Kidney	
Rats + *T. g* (dpi)	No.	p value	No.	p value	No.	p value	No.	p value	No.	p value	No.	p value	No.	p value
WT-SD rats + RH/GFP (10 d)	0/10	1	**9/10**	**<0.001**	0/10	1	0/10	1	**2/10**	0.500	**8/10**	**0.007**	0/10	1
iNOS$^{-/-}$-SD rats + RH/GFP (10 d)	0/6		0/6		0/6		0/6		0/6		0/6		0/6	
WT-SD rats + RH/GFP (20 d)	0/10	1	**6/10**	**0.034**	0/10	1	0/10	1	0/10	**1**	**5/10**	0.093	0/10	1
iNOS$^{-/-}$-SD rats + RH/GFP (20 d)	0/6		0/6		0/6		0/6		0/6		0/6		0/6	
WT-SD rats + RH/GFP (30 d)	0/10	1	**2/10**	0.500	0/10	1	0/10	1	0/10	1	0/10	1	0/10	1
iNOS$^{-/-}$-SD rats + RH/GFP (30 d)	0/6		0/6		0/6		0/6		0/6		0/6		0/6	
WT-SD rats + PLK/RED (60 d)	0/9	1	**4/9**	0.082	0/9	1	0/9	1	0/9	1	0/9	1	0/9	1
iNOS$^{-/-}$-SD rats + PLK/RED (60 d)	0/9		0/9		0/9		0/9		0/9		0/9		0/9	
WT-SD rats + Tgctsd1 (60 d)	0/9	1	**3/9**	0.206	0/9	1	0/9	1	0/9	1	0/9	1	0/9	1
iNOS$^{-/-}$-SD rats + Tgctsd1 (60 d)	0/8		0/8		0/8		0/8		0/8		0/8		0/8	
WT-SD rats + PBS (30 d)	0/6		0/6		0/6		0/6		0/6		0/6		0/6	

The number of *T. gondii* positive/tested rats is shown. Half a gram tissue from each rat was removed, homogenized, and then intraperitoneally injected into a Swiss Webster mouse. Data were analyzed using the Fisher's exact test. Significance was accepted at <0.05, No., number of positive organs detected.

surprisingly the knockout rat PMs showed a strong resistance to *T. gondii* infection even without IFN-γ stimulation (Figures 2A and 2B). In contrast, the *T. gondii* grew well in freshly harvested WT-SD rat PMs, unless rat PMs were pre-treated with IFN-γ, LPS, or sodium nitroprusside (SNP) (Figures 2A and 2C). These findings were confirmed by experiments with the *T. gondii* PLK/RED strain in rat PMs (Figures S3D–S3F) and bone marrow-derived macrophage cells (Figures S3G and S3H). When the NO content in medium supernatants was assayed, the NO level in the WT-SD rat PMs group was positively correlated with *T. gondii* growth inhibition, which could be enhanced by the presence of an NO donor compound SNP (Figures 2A and 2C), while results from the *iNOS*$^{-/-}$-SD groups still showed a strong resistance to *T. gondii* infection no matter whether NO was present or not (Figure S2).

iNOS$^{-/-}$-SD rat PMs infected with *T. gondii* infection caused ROS upregulation and superoxide dismutase 2 depletion

NO, representing reactive nitrogen species (RNS) can synergistically work with reactive oxygen species (ROS) to create a variety of intermediates (Nathan and Shiloh, 2000). Therefore, we wondered about the status of ROS in the macrophages prepared freshly from the *iNOS*$^{-/-}$-SD rats. Our results clearly showed a significant increase of ROS levels in the *iNOS*$^{-/-}$-SD rat PMs within 1 h post-infection (hpi) with *T. gondii* which was even higher than the naturally higher levels of ROS found in the, naturally *Toxoplasma* resistant, LEW rat PMs. Meanwhile, an increase was not detected in the WT-SD rat PMs (Figures 2D and 2E). Importantly, reduced glutathione (GSH), an intracellular antioxidant (also referred to as a cellular ROS scavenger), was also found to be significantly increased in parallel with the levels of ROS (Figure 2F), indicating an oxygen stress response in the infected cells.

Around 95–98% of ROS production is considered to be attributed to the electron transport chain in mitochondria (Skulachev, 1999), and one of the ROS cleaners in mitochondria, superoxide dismutase 2 (SOD2), was detected. Not surprisingly, a dramatic depletion of SOD2 protein was demonstrated by Western blotting in the *iNOS*$^{-/-}$-SD rat PMs infected with *T. gondii* (Figure 2G). To confirm the role of ROS and SOD2 in the *iNOS*$^{-/-}$-SD rat PMs, GSH and Mn (III) tetrakis (4-benzoic acid) porphyrin (MnTBAP (III)) (the superoxide scavenger) were added into the cell culture medium. As expected, ROS stress was alleviated by GSH, MnTBAP (III), or both and resulted in a significant increase in the proliferation of *T. gondii* in the *iNOS*$^{-/-}$-SD rat PMs (Figure 2I). A similar result was observed for PMs from LEW rats (Figure 2J), but not in the WT-SD rat PMs (Figure 2H).

Effect of *T. gondii* infection on the parasitophorous vacuole membrane and mitochondria of *iNOS*$^{-/-}$-SD rat PMs

The parasitophorous vacuole membrane (PVM) is a key barrier required for parasite survival within the host cell (Molestina and Sinai, 2005; Sinai and Joiner, 1997; Suss-Toby et al., 1996). ROS are very important

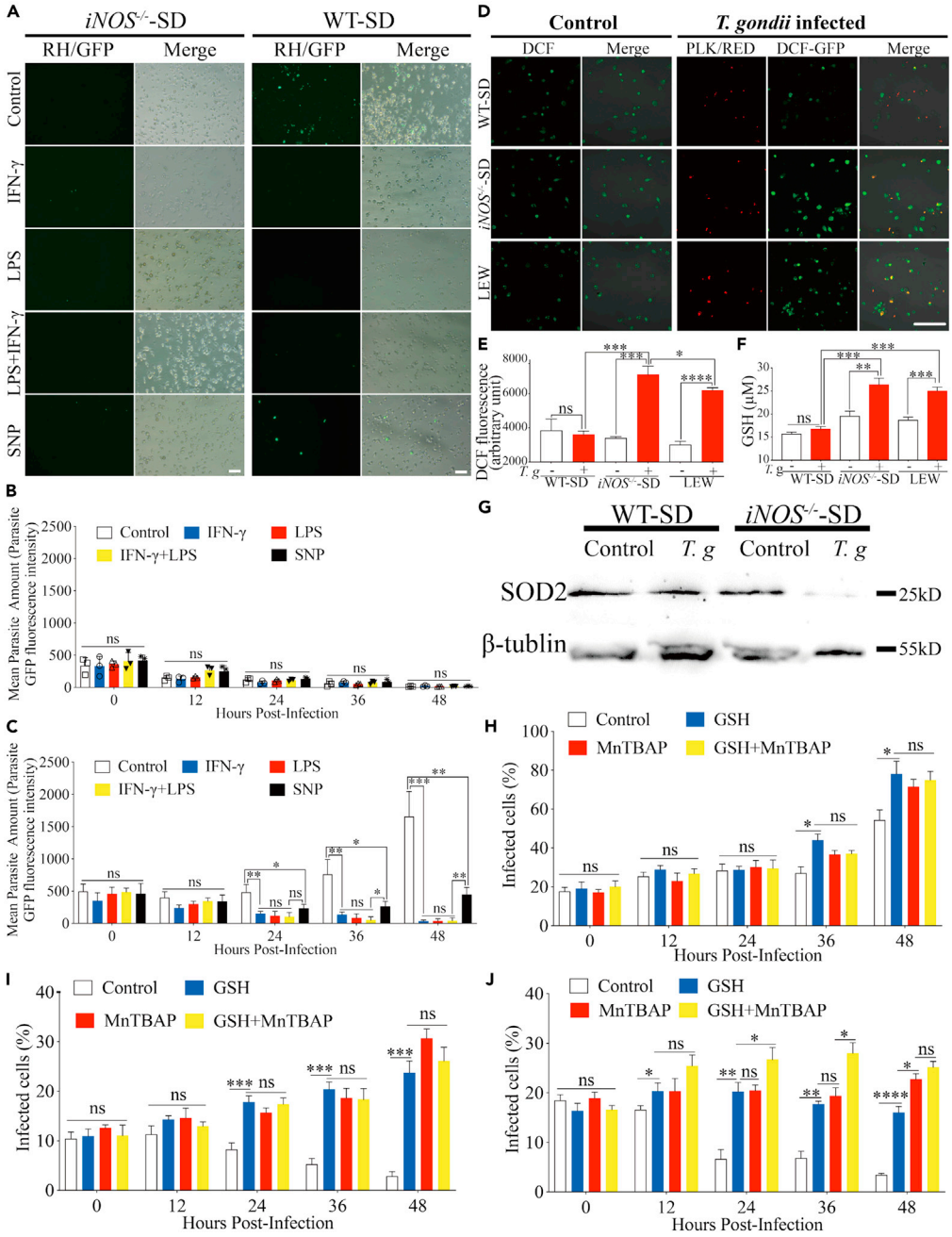

Figure 2. Resistance of *iNOS*$^{-/-}$-SD rats to *T. gondii* is dependent on PMs and ROS bursts

(A) The status of *T. gondii* RH/GFP strain tachyzoites in the *iNOS*$^{-/-}$-SD and WT-SD rat PMs treated with different compounds 48 hours post-infection (hpi), scale bars equal 50 μm. LPS, lipopolysaccharide; IFN-γ, interferon-gamma; SNP, sodium nitroprusside.

(B and C) The mean parasite loads, judged by fluorescence intensity, in *iNOS*$^{-/-}$-SD (B) and WT-SD (C) rat PMs; MOI = 2, cells were transferred into 24-well plates for further experimentation, 5×10^5 cells per well, in triplicate, n = 3.

(D) Detection of *T. gondii* tachyzoites and ROS in rat PMs infected *T. gondii*. Rat PMs were transferred to confocal dishes, 10^6 per dish with or without *T. gondii* PLK/RED strain tachyzoites at an MOI = 2 for 1 h and then washed with 1×PBS 3 times, incubated in RPMI-1640 for 1 hour, followed by another 30-min incubation with DCFH-DA (2′,7′-dichlorofluorescin diacetate) at 10 μM. The resulting oxidized form (DCF) was observed by confocal microscopy, bar = 50 μm.

(E) The oxidized DCF in the rat PMs was detected by flow cytometry. Rats were i.p. infected with 10^7 *T. gondii* PLK/RED strain tachyzoites and then 1 h later rat PMs were collected following i.p. injection with 0.5 mL of PBS and subjected to flow cytometry (n = 3, >10,000 counts).

Figure 2. *Continued*

(F) The GSH level in the rat PMs. Rat PMs were harvested as above but at a later time point (3 hpi); n = 3.

(G) The protein level of SOD2 was measured by Western blotting. Rat PMs were harvested at 3 hpi as above; β-tubulin was performed on the same blot and used to normalize the signal.

(H, I and J) The infection rate of *T. gondii* RH/GFP strain tachyzoites in the WT-SD (H), *iNOS*$^{-/-}$-SD (I), and LEW (J) rat PMs cultured with or without MnTBAP and GSH. Cells were transferred into 24-well plates for subsequent investigation, 5×10^5 per well; MOI = 2; in triplicate, n = 3. All data are presented as mean ± SD and are representative of three independent experiments. *, p < 0.05; **, p < 0.01; ***, p < 0.001; ****, p < 0.0001; ns: no significant difference. See also Figures S2, S3, S5, and S6.

effectors in the host cellular immune response to intracellular pathogens, which need to cross the PVM to be able to damage *T. gondii*. When we monitored the structure of the PVM in the infected cells 3 hpi by transmission electron microscopy, the resulting images clearly revealed that the structure of the PVM in *iNOS*$^{-/-}$-SD rat PMs was blurred and damaged (Figures 3C and 3D, red arrows). However, the PVMs of WT-SD rat PMs were structurally clear (Figures 3A and 3B, white arrows). ROS is considered a double-edged molecule; it is not only toxic to parasites but also damage host cells (Zhang et al., 2016). The mitochondrial membranes in the *iNOS*$^{-/-}$-SD rat PMs infected with *T. gondii* were found to be scattered, be distorted, and lacked intact internal structures (Figure 3G, red arrows). In contrast, the uninfected *iNOS*$^{-/-}$-SD rat PMs' and infected/uninfected WT-SD rat PMs' mitochondria appeared normal (Figures 3E, 3F, and 3H, black arrows). The damage in the infected *iNOS*$^{-/-}$-SD rat PMs might be the consequences of specific ROS bursts in the infected cells. These results suggested that the burst of ROS might be the key reason for PVM and host mitochondrion disruption in the *iNOS*$^{-/-}$-SD rat PMs infected with *T. gondii*.

Rapid cell death and pyroptosis in the *iNOS*$^{-/-}$-SD rat PMs infected with *T. gondii*

As revealed by propidium iodide (PI) and Hoechst staining, *T. gondii* infection was found to induce cell death in all freshly collected rat PMs tested from different strains of rats, especially in the *iNOS*$^{-/-}$-SD rat PMs (which increased up to 22%–31%) (Figures 4A and 4B). Data from flow cytometry analysis also confirmed these findings. This result further supported the observations that the major proportion of cell death was necrosis both in the LEW and *iNOS*$^{-/-}$-SD rat PMs (Figure 4C). We then investigated the expression of pyroptosis-specific markers including caspase-1, IL-1β, and IL-18 by Western blotting. The results showed that pro-caspase-1, the precursor of caspase-1, remained unchanged in the rat PMs post-infection, while the mature form caspase-1-p12 and the downstream cytokines IL-1β and IL-18 were found to be increased in the *iNOS*$^{-/-}$-SD and LEW rat PMs when infected with *T. gondii* (Figures 4D and 4E). These findings were further confirmed by using an inhibitor (VX765) of caspase-1 which protected *T. gondii* from damage and resulted in a higher infection ratio (Figure S4). In contrast, however, the caspase-3-p12, a specific signal for apoptosis, was not detected (Figure 4D). Furthermore, treatment to inhibit the activity of caspase-3-p12 by affecting a rat-specific upstream protein NLRP3 using the inhibitor MCC950 resulted in no change in infection ratio compared with the control in the *iNOS*$^{-/-}$-SD and LEW rat PMs (Figure S4). Taken together, these results clearly support the cell fate as pyroptosis but not apoptosis in the *iNOS*$^{-/-}$-SD rat PMs infected with *T. gondii*. Thus, the explanation for the complete resistance to *T. gondii* infection found in the *iNOS*$^{-/-}$-SD rat is related to cell pyroptosis as a mechanism. This raises a further critical question as to how *T. gondii* infection can cause pyroptosis in the PMs of the *iNOS*$^{-/-}$-SD rat.

Effect of GRA43 on the induction of pyroptosis in *iNOS*$^{-/-}$-SD rat PMs

Previous studies suggested that GRAs such as GRA43 are linked to pyroptosis in LEW rat macrophages (Wang et al., 2019a). To test if these proteins were the main cause of pyroptosis in the PMs of *iNOS*$^{-/-}$-SD rat, we generated a *GRA43* knockout *T. gondii* strain (RH-Δ*gra43*) which was then used to infect the rat PMs from different rat strains. Results clearly indicated that RH-Δ*gra43* strain indeed produced a significantly higher infection ratio in the PMs of *iNOS*$^{-/-}$-SD and LEW rats than those found in the parental RH strain (Figures S5B and S5C). Furthermore, our results also demonstrated that the RH-Δ*gra43* strain caused much less ROS in the PMs of *iNOS*$^{-/-}$-SD and LEW rats (Figures S5D and S5E). However, this effect was not observed in the *iNOS*$^{-/-}$-SD rat PMs infected with the RH-*Δrop18* strain (Figure S6). These results indicate that *T. gondii* GRA43 is a key trigger for causing the pyroptosis in the *iNOS*$^{-/-}$-SD rat PMs.

DISCUSSION

The biological functions of NO have been extensively investigated, and the effect of this molecule against pathogens is also well understood. A large number of early studies based on mouse and rat models have

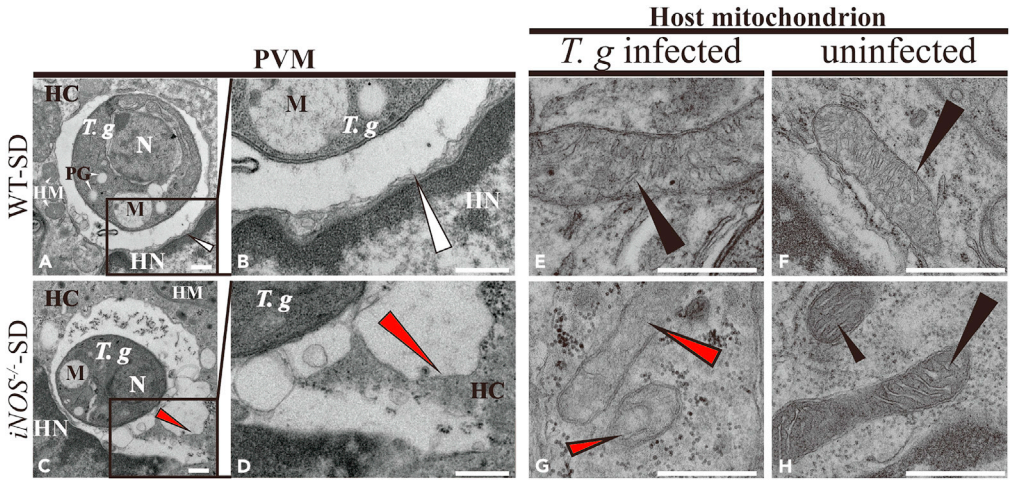

Figure 3. The ultrastructure of the parasitophorous vacuole membrane (PVM) and host mitochondrion in the WT and *iNOS*$^{-/-}$-SD rat PMs infected with *T. gondii*

(A–D) The PVM structures of WT-SD rat PMs infected with *T. gondii* are normally clearly seen with a double membrane (A, B, white arrows), while blurred membranes in PVMs were observed in the *iNOS*$^{-/-}$-SD rat PMs infected with this parasite (C, D, red arrows).

(E–H) The host mitochondrial morphology in PMs from WT (E, F) and *iNOS*$^{-/-}$-SD (G, H) with or without *T. gondii* infection. Intact membranes with clear outer double membranes and internal ridges were observed in WT SD PMs infected with or without *T. gondii* (E,F, black arrows) and in *iNOS*$^{-/-}$-SD PMs without *T. gondii* infection (H, black arrows), while blurred inner membranes were found in the *iNOS*$^{-/-}$-SD PMs infected with *T. gondii* (G, red arrows). Rat PMs were obtained at 3 hpi, rats aged 4 weeks had 10^7 *T. gondii* PLK/RED strain tachyzoites i.p. injected. HC, host cell; HM, host cell mitochondrion; HN, host cell nucleus; N, *T. gondii* nucleus; PG, polysaccharide granules; M, *T. gondii* mitochondrion; bar = 500 nm.

shown that NO produced by iNOS is a critical anti-*T. gondii* host factor (Alexander et al., 1997; Li et al., 2012; Zhao et al., 2013). In addition, our earlier studies in rats also indicated that NO played an important role against *Leishmania* and *Schistosoma* infections (Chen, 2016; Shen et al., 2017a, b).

To our surprise, however, the *iNOS*$^{-/-}$-SD rat was found to be extremely resistant to *T. gondii* infection resulting in failure to form cysts and to cause active infection. Traditionally, mice macrophages were found to be more susceptible to *T. gondii* infection if the *iNOS* gene was knocked out or inhibited (Alderton et al., 2001; Scharton-Kersten et al., 1997). This demonstrated that iNOS or NO played an essential role in protecting mice from toxoplasmosis (Alexander et al., 1997). Unlike mice, rats are relatively resistant to *T. gondii* infection with different rat strains showing different rates of survival and tissue cyst formation (Freyre et al., 2003a, 2003b, 2004; Gao et al., 2015; Zenner et al., 1993). Once infected, despite strain variation, most rats remain asymptomatic and usually develop only a chronic infection with the production of cysts (Gao et al., 2015). This has been attributed to the high levels of expression of iNOS and high concentrations of NO in rats (Li et al., 2012). For example, with a lower iNOS expression and lower NO level, BN rats are more susceptible to *T. gondii* infection than the high iNOS expression and high NO levels found in LEW rats (Li et al., 2012). Our results, however, demonstrated that the *iNOS*$^{-/-}$-SD rat showed a resistance to *T. gondii* infection that was dramatically high. This result was unexpected and surprising to us. Further characterization showed a significant increase of ROS in the *iNOS*$^{-/-}$-SD rats infected with *T. gondii* and suggested that ROS was linked to this resistance. Previous studies indicated that the macrophages from BN rats exhibited much lower levels of ROS than LEW rat PMs (Witola et al., 2017). Interestingly, although the expression of the iNOS gene and the levels of NO were lower in the SD rat PMs than those found in the LEW rat (Gao et al., 2015), our results show that the ROS levels in both SD and LEW rat PMs are similar. Therefore, it seems that the different expression levels of iNOS or the amount of NO are linked to the differences in susceptibility of the SD and LEW rats against *T. gondii* infection and are therefore the key determinants of innate susceptibility/resistance. However, our results from the *iNOS*$^{-/-}$-SD rats contradicted this because both *iNOS*$^{-/-}$-SD and LEW rats showed similar resistance to *T. gondii* infection. These observations implied that there is the existence or activation of a hidden and aggressive immune mechanism in SD rats, active against *T. gondii* infection, when iNOS was absent.

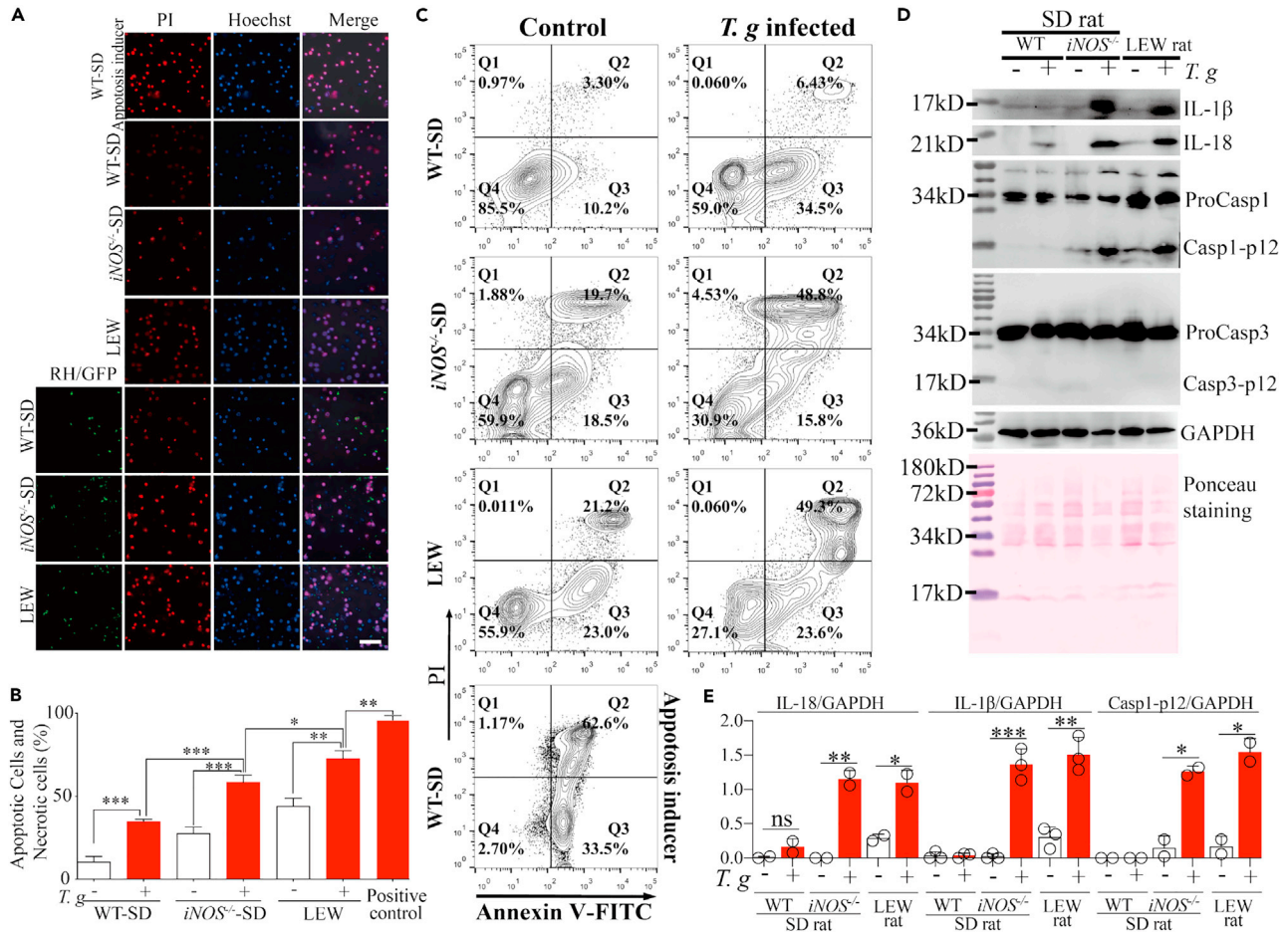

Figure 4. Viability of rat PMs and cell death pattern protein expression

(A and B) Cell death of rat PMs, including apoptosis and necrosis, post-infection with the *T. gondii* RH/GFP strain, as judged by PI and Hoechst co-staining and confocal microscopy (A) followed by quantification (B). MOI = 2, cells were transferred to confocal plates or 24-well plates, 5×10^5 per well; >300 rat PM counts, in triplicate; n = 3, bar = 50 μm.

(C) Representative flow cytometry dot plots of rat PMs stained with PI and Annexin V-FITC. Rat PMs were either uninfected (medium) or infected with *T. gondii* for 4 h and compared with rat PMs treated with the apoptosis inducer (Beyotime, China, lot#C0005) for 4 h, MOI = 2, >10,000 counts.

(D) Western blot analyses of expression of IL-1β, IL-18, caspase-1, and caspase-3 in rat PM lysates. Rat PMs were infected with *T. gondii* 10^7 RH/GFP tachyzoites at 3 hpi; GAPDH was performed in parallel using the same set of samples for normalizing expression; Ponceau staining was performed before caspase-1 analysis.

(E) Quantification of Western blots, including IL-1β (n = 3), IL-18 (n = 2), and Casp1-p12 (n = 2). The protein bands were densitometrically quantified, and the relative amounts of expressed IL-18, IL-1β, and the cleavage caspase-1 (Casp1-p12) protein normalized against GAPDH using ImageJ. All data are presented as mean ± SD. *, $p < 0.05$; **, $p < 0.01$; ***, $p < 0.001$. See also Figures S4 and S7.

Owing to the significant increase of ROS found in freshly collected *iNOS*$^{-/-}$-SD PMs, infected with *T. gondii*, we thought that ROS might play a role in this resistance in the *iNOS*$^{-/-}$-SD rat. It is well known that ROS, produced by oxidases and nonenzymatic sources, are highly reactive metabolites of molecular oxygen and comprise hydrogen peroxide, superoxide radicals, and hydroxyl radicals (Andreyev et al., 2005). These molecules have wide biological functions in different animals from invertebrates to humans, and one important role is in host defense against intracellular pathogens ranging from viruses to parasites. The generation of ROS was found to limit the survival and proliferation of *T. gondii* in infected mammalian cells (Aline et al., 2002; Buzoni-Gatel and Werts, 2006; Miller et al., 2006; Murray et al., 1985). However, ROS molecules are a double-edged sword. They can kill pathogens and also damage host cell lipids, DNA, RNA, and proteins, resulting in cellular damage and even cell death (Aicardo et al., 2016). Although the effect of ROS against *T. gondii* had been reported in the LEW rat (Cavailles et al., 2014; Witola et al., 2017), in the early stages of this work it was hard for us to understand the nature of the mechanism (or reason) for this increased ROS in the infected *iNOS*$^{-/-}$-SD rat macrophages. From electron microscopy and cell culture

observations, we found damaged PVMs and disruption of host cell mitochondria as well as increased cell death in the infected *iNOS*$^{-/-}$-SD rat PMs. These observations were linked to the increase of ROS in the infected cells because similar results were not observed in the PMs isolated from infected WT-SD rats. Clearly, ROS are the main factor for the death of cells and the parasite in the infected PMs. They not only are toxic to the PVM of *T. gondii* tachyzoites but can also damage the host cell mitochondrion and subsequently cause cell death. Several studies have demonstrated that serious mitochondrial damage always accompanies cell death (Fan et al., 2017; Wang et al., 2019b). Other studies have shown that removal of oxidants by MnTBAP(III) in LEW macrophages leads to a significant increase in cells containing tachyzoites and is accompanied by a decreased resistance to *T. gondii* infection (Witola et al., 2017). Our results also demonstrated the presence of more parasites and less cell death in infected *iNOS*$^{-/-}$-SD rat PMs when treated with MnTBAP(III) or GSH. Therefore, the innate response, by rapid killing of *T. gondii* tachyzoites, in the *iNOS*$^{-/-}$-SD rat PMs is dependent on the highly active ROS but is countered by the high cost of host cell death. This suggests that a two-level defense system may exist in rats: an *iNOS*-based system that drives the normal response against pathogens but causes minimal host damage and a much more self-destructive, ROS-based, system that kicks in if *iNOS* is absent or perhaps fails to cope with the infection.

This raises the question as to how ROS is upregulated in the macrophages of infected *iNOS*$^{-/-}$-SD rats. Interestingly, other studies showed that the resistance of the LEW rat was linked to inherently high transcript levels of Cyp2d3, Cyp25, and Cybrd1 (Witola et al., 2017), whose gene products promote mitochondrial electron transfer, the Fenton reaction, and generate large amounts of ROS (Hrycay and Bandiera, 2015). However, high levels of these corresponding enzymes were not found in the *iNOS*$^{-/-}$-SD rat PMs infected with *T. gondii* (NCBI number: PRJNA642722), which suggests that other unknown pathways related to the upregulation of ROS must exist in this *iNOS*$^{-/-}$-SD rat. Based on the comparison of metabolic pathways between WT and *iNOS*$^{-/-}$-SD rats, no significant differences were found (data not shown). We thought, therefore, that perhaps other factors, derived from *T. gondii*, might cause the upregulation of ROS in *iNOS*$^{-/-}$-SD rats. It has been reported that ROPs and GRAs play an extremely important function in the invasion and development of *T. gondii* in the host cell (Gold et al., 2015). Among them, some have been investigated well. GRA43 is a dense granule protein colocalized with GRA7 and can influence the correct localization of other GRAs to the PVM, a key requirement for the development of *T. gondii* within the host cell (Wang et al., 2019a). GRA7 is a transmembrane protein secreted from *T. gondii* that was considered to interact with ROP complexes in the host cytosol and play a critical role in MyD88-dependent TRAF6 activation and ROS production in macrophages (Alaganan et al., 2014; Yang et al., 2016). By comparison with the freshly collected WT-SD rat PMs infected with *T. gondii*, our data showed that the *iNOS*$^{-/-}$-SD rat PMs infected with *T. gondii* presented higher transcript levels of MyD88 and TRAF6 (Table S1), followed by a burst of ROS and the killing of the parasite in the *iNOS*$^{-/-}$-SD rat PMs. However, after the knockout of GRA43, the *T. gondii-Δgra43* tachyzoites failed to induce the upregulation of ROS in *iNOS*$^{-/-}$-SD rat PMs, while the *T. gondii-Δgra43* strain could proliferate intracellularly. These results demonstrated that the GRA43 might interfere with the extension of GRA7 into the host cytosol resulting in a failure to induce the host ROS burst in *iNOS*$^{-/-}$-SD rat PMs. Moreover, the accumulation of ROS in macrophages is considered to be closely related to the amount of NO content in cells. Studies indicated that NO produced by iNOS could promote the accumulation of SOD2, one of the major mitochondrial antioxidants that can significantly suppress the ROS (Kaneko et al., 2012). Therefore, iNOS or NO depletion may eliminate the suppression and uplift the ROS, followed by the ROS depletion by SOD2 in a manner similar to our observations in the *iNOS*$^{-/-}$-SD rat PMs infected with *T. gondii*. However, the supply of NO to the *iNOS*$^{-/-}$-SD rat PMs in vitro did not block the ROS anti-*T. gondii* pathway, which excluded the direct role of NO in ROS suppression. Indeed, it was shown that the iNOS monomer could be localized to the peroxisome which, in turn, was believed to alleviate damaging nitrogen or oxygen radicals (Loughran et al., 2005; Stolz et al., 2002). This may explain why TRAF6 and MyD88 were upregulated in WT-SD rat PMs infected with *T. gondii*, compared with the uninfected WT-SD rat PMs, but that the ROS did not increase significantly. Therefore, we conclude that the absence of iNOS and the normal secretion of *T. gondii* GRA7 jointly promoted the ROS burst and that the burst of ROS not only was toxic to the parasite but also damaged the host cell mitochondrion and resulted in the depletion of SOD2. In addition, we also observed the depletion of SOD2 in the *iNOS*$^{-/-}$-SD rat PMs. SOD2 can banish superoxides (O_2^{2-}) and reduce the mitochondrial membrane oxidation pressure (Becana et al., 1986). In other words, the depletion of SOD2 may act in a parallel way to uplift ROS.

ROS production in macrophages is always related to inflammasome activation, which may directly cause cellular damage, oxidative stress, and pyroptotic processes (Shen et al., 2020; Wang et al., 2019b).

Pyroptosis in pathogen restriction is a critical innate immune response to prevent intracellular infection (Boucher et al., 2015). It is emerging as an important mechanism of microbial clearance, during which the activation of caspase-1 leads to the production of IL-1β and IL-18 (Boucher et al., 2015; Xia et al., 2019). In LEW rat macrophages, *T. gondii* infection could activate the NLRP1 inflammasome, secretion of mature IL-1β, resulting in pyroptosis, and inhibition of parasite replication (Cavailles et al., 2014; Cirelli et al., 2014; Ewald et al., 2014). Subsequent research has confirmed that three dense granule proteins (GRAs) promote parasite-stimulated pyroptosis in LEW rat macrophages (Wang et al., 2019a). Our results directly show that the *iNOS*$^{-/-}$-SD rat PMs infected with *T. gondii* could induce cell pyroptosis; however, when the GRA43 protein is absent, the resistance to *T. gondii-Δgra43* was decreased in *iNOS*$^{-/-}$-SD rat PMs. Pyroptosis in *iNOS*$^{-/-}$-SD rat PMs may only be limited to *T. gondii*, or other apicomplexans, which carry out active invasion and secrete GRA proteins but not to those that adopt passive invasion like *Leishmania amazonensis* (LV78) (Chen, 2016) by phagocytosis. Another well-known virulence factor in *T. gondii*, rhoptry protein ROP18, did not seem to be involved in the activation of ROS/NLRP1 resistance as found previously in the LEW rat (Cavailles et al., 2014).

In summary, our studies have potentially uncovered a novel, non-traditional, innate immune pathway in the *iNOS* knockout SD rat which, in the absence of iNOS, enables complete resistance to *T. gondii* infection (Figure S7). This resistance mechanism is mainly dependent on the upregulation of ROS and subsequent pyroptosis in rat PMs. The activation of the ROS/NLRP1 pathway requires the secretion of the *T. gondii* GRA43 protein. Because WT-SD rats are incapable of activating the ROS/NLRP1 pathway, iNOS is considered to be an essential negative factor that modulates the pathway into a pre-activated state. Hence, in the SD rat, there exists a dormant powerful, but suicidal pathway, of pyroptosis that is specific to *T. gondii* and is locked down by iNOS. This finding may inspire some future novel therapeutic strategies for the prevention of domestic livestock or human toxoplasmosis and, possibly, other infectious diseases.

Limitations of the study

Owing to the limitations on the usage of animals, the detection of the parasite at earlier time points, during the acute stage of infection within the first 10 days, was not performed. As a result, we were unable to compare parasite burdens between WT and *iNOS*$^{-/-}$-SD rats in the very early stages of infection, nor were we able to directly demonstrate the anti-tachyzoite capability of the peritoneal macrophages obtained during the acute stage.

For in vitro experiments, a high level of IFN-γ (100 ng/mL) was used in the positive controls. We recognize that this does not directly reflect the physiological levels measured in in vivo sera (averaging 200–400 pg/mL) (Figure S1). However, we used these higher levels, in the in vitro functional assays, to show the proof of concept that WT rat macrophages can eliminate *T. gondii* in an IFN-γ-dependent manner. By contrast, in the knockout mutant, rat macrophages could eliminate the parasite even in the absence of IFN-γ. We recognize that it would be desirable to match the IFN-γ concentrations in in vitro and in vivo experiments. However, the range of physiological in vivo values of IFN-γ concentration can vary widely in different hosts, such as mice, rats, and humans, and is dependent on immunological status. Even in our own study just on rats alone (Figure S1), the ranges of IFN-γ concentrations varied between 50 and 600 pg/mL in the WT rats, depending on the immunological status. Furthermore, in vivo concentrations of IFN-γ are often only measured as average values, while in reality, there will be localized variations in the microenvironments of individual macrophages (which, of course, produce IFN-γ themselves). While we recognize the desirability of closely matching IFN-γ concentrations in in vitro and in vivo experiments, we believe that this does not have an impact on the overall conclusions of our study.

Throughout the study, we used peritoneal macrophages that were freshly collected before being exposed to a variety of experiments. These freshly isolated macrophages are in a similar physiological condition and show most of the physiological functions of in vivo macrophages. We believe that this accurately represents what is happening to these macrophages in vivo; however, we do recognize the possibility that these cells may have altered behavior once harvested. We recognize that further work may be needed to fully establish the link between the in vitro and in vivo experiments.

While we have demonstrated that GRA43 triggered the *T. gondii* resistance pathway in *iNOS*$^{-/-}$-SD rat PMs, we recognize that some other GRAs and secreted proteins may also contribute to the initiation of

T. gondii resistance. Therefore, further studies are needed to better understand the full story with respect to the detailed identities of these resistance triggers.

STAR★METHODS

Detailed methods are provided in the online version of this paper and include the following:

- KEY RESOURCES TABLE
- RESOURCE AVAILABILITY
  - Lead contact
  - Materials availability
  - Date and code availability
- EXPERIMENTAL MODEL AND SUBJECT DETAILS
- METHOD DETAILS
  - Animals and parasites
  - Chemicals
  - Antibodies
  - *In vivo* parasite infection and bioassay
  - Histological analysis of brain tissue sections
  - Preparation of primary fibroblasts, peritoneal macrophages and bone marrow derived macrophages
  - Treatments of rat cells and parasite infection
  - Determination of nitric oxide (NO), reactive oxygen species (ROS) and glutathione (GSH)
  - Sample preparation for transmission electron microscopy
  - Western-blotting
  - Determination of the effect of GSH and MnTBAP on the growth of *T. gondii* in SD and LEW RPMs
  - Cell viability assay
  - GRA43 knock-out and cell infection
  - Immunofluorescence assays (IFA)
  - Determination of ROS in RPMs infected with the *T. gondii* RH-Δ*gra43*
  - RNA extraction, library preparation and RNA sequencing
- QUANTIFICATION AND STATISTICAL ANALYSIS

SUPPLEMENTAL INFORMATION

Supplemental information can be found online at https://doi.org/10.1016/j.isci.2021.103280.

ACKNOWLEDGMENTS

We thank Prof. Xue-Nan Xuan, Obihiro University of Agriculture and Veterinary Medicine, who kindly provided the RH/GFP and PLK/RED strains of *T. gondii*. We also thank Prof. Jian-Du, Anhui Medical University, who provided the RH-Δ*rop18* strain of *T. gondii*. This work was supported by the National Key R&D Program of China (2017YFD0500400 to Z.R.L. and D.H.L.), National Natural Science Foundation of China (31772445 to D.H.L.), and University of Salford (to G.H.).

AUTHOR CONTRIBUTIONS

Conceptualization: ZRL and DHL; methodology: ZRL, DHL, and ZJW; formal analysis: ZJW, DHL, GH, and MY; Investigation: ZJW, SMY, JMG, and PZ; visualization: ZJW and DHL; project administration: ZRL and DHL; funding acquisition: ZRL, DHL, and GH; Writing – original draft: ZJW, DHL, and ZRL; Writing – review & editing: ZJW, GH, MY, DHL, and ZRL.

DECLARATION OF INTERESTS

The authors declare no competing interests.

Received: November 16, 2020
Revised: March 8, 2021
Accepted: October 13, 2021
Published: November 19, 2021

REFERENCES

Aicardo, A., Martinez, D.M., Campolo, N., Bartesaghi, S., and Radi, R. (2016). Biochemistry of nitric oxide and peroxynitrite: sources, targets and biological implications. In Biochemistry of Oxidative Stress (Springer International Publishing), pp. 49–77. https://doi.org/10.1007/978-3-319-45865-6_5.

Alaganan, A., Fentress, S.J., Tang, K., Wang, Q., and Sibley, L.D. (2014). *Toxoplasma* GRA7 effector increases turnover of immunity-related GTPases and contributes to acute virulence in the mouse. Proc. Natl. Acad. Sci. U S A *111*, 1126–1131. https://doi.org/10.1073/pnas.1313501111.

Alderton, W.K., Cooper, C.E., and Knowles, R.G. (2001). Nitric oxide synthases: structure, function and inhibition. Biochem. J. *357*, 593–615. https://doi.org/10.1042/0264-6021:3570593.

Alexander, J., Scharton-Kersten, T.M., Yap, G., Roberts, C.W., Liew, F.Y., and Sher, A. (1997). Mechanisms of innate resistance to *Toxoplasma gondii* infection. Philosophical Trans. R. Soc. B: Biol. Sci. *352*, 1355–1359. https://doi.org/10.1098/rstb.1997.0120.

Aline, F., Bout, D., and Dimier-Poisson, I. (2002). Dendritic cells as effector cells: gamma interferon activation of murine dendritic cells triggers oxygen-dependent inhibition of *Toxoplasma gondii* replication. Infect. Immun. *70*, 2368–2374. https://doi.org/10.1128/IAI.70.5.2368-2374.2002.

Andreyev, A.Y., Kushnareva, Y.E., and Starkov, A.A. (2005). Mitochondrial metabolism of reactive oxygen species. Biokhimiya *70*, 246–264. https://doi.org/10.1007/s10541-005-0102-7.

Becana, M., Aparicio-Tejo, P., Irigoyen, J.J., and Sánchez-Díaz, M. (1986). Some enzymes of hydrogen peroxide metabolism in leaves and root nodules of *Medicago sativa*. Plant Physiol. *82*, 1169–1171. https://doi.org/10.2307/4270348.

Behnke, M.S., Dubey, J.P., and Sibley, L.D. (2016). Genetic mapping of pathogenesis determinants in *Toxoplasma gondii*. Annu. Rev. Microbiol. *70*, 63–81. https://doi.org/10.1146/annurev-micro-091014-104353.

Bogdan, C. (2001). Nitric oxide and the immune response. Nat. Immunol. *2*, 907–916. https://doi.org/10.1038/ni1001-907.

Boucher, D., Chen, K.W., and Schroder, K. (2015). Burn the house, save the day: pyroptosis in pathogen restriction. Inflammasome *2*, 1–6. https://doi.org/10.1515/infl-2015-0001.

Buzoni-Gatel, D., and Werts, C. (2006). *Toxoplasma gondii* and subversion of the immune system. Trends Parasitol. *22*, 448–452. https://doi.org/10.1016/j.pt.2006.08.002.

Cavailles, P., Flori, P., Papapietro, O., Bisanz, C., Lagrange, D., Pilloux, L., Massera, C., Cristinelli, S., Jublot, D., Bastien, O., et al. (2014). A highly conserved *Toxo1* haplotype directs resistance to toxoplasmosis and its associated caspase-1 dependent killing of parasite and host macrophage. PLoS Pathog. *10*, e1004005. https://doi.org/10.1371/journal.ppat.1004005.

Chen, F., Li, Q., Zhang, Z., Lin, P., Lei, L., Wang, A., and Jin, Y. (2015). Endoplasmic reticulum stress cooperates in zearalenone-induced cell death of RAW 264.7 macrophages. Int. J. Mol. Sci. *16*, 19780–19795. https://doi.org/10.3390/ijms160819780.

Chen, Y. (2016). *Leishmania amazonensis* Infection in Mouse and Rat Model: The Mechanism of Host Specificity (Sun Yat-Sen University).

Cirelli, K.M., Gorfu, G., Hassan, M.A., Printz, M., Crown, D., Leppla, S.H., Grigg, M.E., Saeij, J.P.J., and Moayeri, M. (2014). Inflammasome sensor NLRP1 controls rat macrophage susceptibility to *Toxoplasma gondii*. PLoS Pathog. *10*, e1003927. https://doi.org/10.1371/journal.ppat.1003927.

Croen, K.D. (1993). Evidence for an antiviral effect of nitric oxide. Inhibition of herpes simplex virus type 1 replication. J. Clin. Invest. *91*, 2446–2452. https://doi.org/10.1172/JCI116479.

Du, J., An, R., Chen, L., Shen, Y., Chen, Y., Cheng, L., Jiang, Z., Zhang, A., Yu, L., Chu, D., et al. (2014). *Toxoplasma gondii* virulence factor ROP18 inhibits the host NF-κB pathway by promoting p65 degradation. J. Biol. Chem. *289*, 12578–12592. https://doi.org/10.1074/jbc.M113.544718.

Dubey, J.P., and Frenkel, J.K. (1998). Toxoplasmosis of rats: a review, with considerations of their value as an animal model and their possible role in epidemiology. Vet. Parasitol. *77*, 1–32. https://doi.org/10.1016/S0304-4017(97)00227-6.

Dupont, C.D., Christian, D.A., and Hunter, C.A. (2012). Immune response and immunopathology during toxoplasmosis. Semin. Immunopathology *34*, 793–813. https://doi.org/10.1007/s00281-012-0339-3.

Ewald, S.E., Chavarria-Smith, J., and Boothroyd, J.C. (2014). NLRP1 is an inflammasome sensor for *Toxoplasma gondii*. Infect. Immun. *82*, 460–468. https://doi.org/10.1128/IAI.01170-13.

Fan, S., Yu, Y., Qi, M., Sun, Z., Li, L., Yao, G., Tashiro, S.I., Onodera, S., and Ikejima, T. (2012). P53-mediated GSH depletion enhanced the cytotoxicity of NO in silibinin-treated human cervical carcinoma HeLa cells. Free Radic. Res. *46*, 1082–1092. https://doi.org/10.3109/10715762.2012.688964.

Fan, W., Shen, T., Ding, Q., Lv, Y., Li, L., Huang, K., Yan, L., and Song, S. (2017). Zearalenone induces ROS-mediated mitochondrial damage in porcine IPEC-J2 cells. J. Biochem. Mol. Toxicol. *31*. https://doi.org/10.1002/jbt.21944.

Flegr, J., Prandota, J., Sovičková, M., and Israili, Z.H. (2014). Toxoplasmosis - a global threat. Correlation of latent toxoplasmosis with specific disease burden in a set of 88 countries. PLoS ONE *9*. https://doi.org/10.1371/journal.pone.0090203.

Freyre, A., Falcón, J., Correa, O., Mendez, J., González, M., Venzal, J.M., and Morgades, D. (2003a). Cyst burden in the brains of Wistar rats fed *Toxoplasma* oocysts. Parasitol. Res. *89*, 342–344. https://doi.org/10.1007/s00436-002-0758-5.

Freyre, A., Falcón, J., Mendez, J., Correa, O., Morgades, D., and Rodríguez, A. (2004). An investigation of sterile immunity against toxoplasmosis in rats. Exp. Parasitol. *107*, 14–19. https://doi.org/10.1016/j.exppara.2004.04.005.

Freyre, A., Falcón, J., Mendez, J., González, M., Venzal, J., and Morgades, D. (2003b). Fetal *Toxoplasma* infection after oocyst inoculation of pregnant rats. Parasitol. Res. *89*, 352–353. https://doi.org/10.1007/s00436-002-0759-4.

Gao, J.M., Xie, Y.T., Xu, Z.S., Chen, H., Hide, G., Yang, T.B., Shen, J.L., Lai, D.H., and Lun, Z.R. (2017). Genetic analyses of Chinese isolates of *Toxoplasma gondii* reveal a new genotype with high virulence to murine hosts. Vet. Parasitol. *241*, 52–60. https://doi.org/10.1016/j.vetpar.2017.05.007.

Gao, J.M., Yi, S.Q., Wu, M.S., Geng, G.Q., Shen, J.L., Lu, F.L., Hide, G., Lai, D.H., and Lun, Z.R. (2015). Investigation of infectivity of neonates and adults from different rat strains to *Toxoplasma gondii* Prugniaud shows both variation which correlates with *iNOS* and Arginase-1 activity and increased susceptibility of neonates to infection. Exp. Parasitol. *149*, 47–53. https://doi.org/10.1016/j.exppara.2014.12.008.

Gauuan, P.J.F., Trova, M.P., Gregor-Boros, L., Bocckino, S.B., Crapo, J.D., and Day, B.J. (2002). Superoxide dismutase mimetics: synthesis and structure-activity relationship study of MnTBAP analogues. Bioorg. Med. Chem. *10*, 3013–3021. https://doi.org/10.1016/S0968-0896(02)00153-0.

Gazzinelli, R.T., Mendonça-Neto, R., Lilue, J., Howard, J., and Sher, A. (2014). Innate resistance against *Toxoplasma gondii*: an evolutionary tale of mice, cats, and men. Cell Host Microbe *15*, 132–138. https://doi.org/10.1016/j.chom.2014.01.004.

Gold, D.A., Kaplan, A.D., Lis, A., Bett, G.C.L., Rosowski, E.E., Cirelli, K.M., Bougdour, A., Sidik, S.M., Beck, J.R., Lourido, S., et al. (2015). The *Toxoplasma* dense granule proteins GRA17 and GRA23 mediate the movement of small molecules between the host and the parasitophorous vacuole. Cell Host Microbe *17*, 642–652. https://doi.org/10.1016/j.chom.2015.04.003.

Griffith, O.W., and Stuehr, D.J. (1995). Nitric oxide synthases: properties and catalytic mechanism. Annu. Rev. Physiol. *57*, 707–734. https://doi.org/10.1146/annurev.ph.57.030195.003423.

Hnasko, T.S., and Hnasko, R.M. (2015). The western blot. In Methods in Molecular Biology, R. Hnasko, ed. (Springer New York), pp. 87–96. https://doi.org/10.1007/978-1-4939-2742-5_9.

Hoffmann, P., Wiesmüller, K.-H., Metzger, J., Jung, G., and Bessler, W.G. (1989). Induction of tumor cytotoxicity in murine bone marrow-derived macrophages by two synthetic lipopeptide analogues. Biol. Chem. Hoppe-Seyler *370*, 575–582. https://doi.org/10.1515/bchm3.1989.370.1.575.

Hrycay, E.G., and Bandiera, S.M. (2015). Involvement of Cytochrome P450 in Reactive Oxygen Species Formation and Cancer, 1st Ed, Advances in Pharmacology (Elsevier Inc). https://doi.org/10.1016/bs.apha.2015.03.003.

Hunter, C.A., and Sibley, L.D. (2012). Modulation of innate immunity by *Toxoplasma gondii*

virulence effectors. Nat. Rev. Microbiol. *10*, 766–778. https://doi.org/10.1038/nrmicro2858.

James, S.L. (1995). Role of nitric oxide in parasitic infections. Microbiol. Rev. *59*, 533–547. https://doi.org/10.1128/MMBR.59.4.533-547.1995.

Kaneko, Y.S., Ota, A., Nakashima, A., Mori, K., Nagatsu, I., and Nagatsu, T. (2012). Regulation of oxidative stress in long-lived lipopolysaccharide-activated microglia. Clin. Exp. Pharmacol. Physiol. *39*, 599–607. https://doi.org/10.1111/j.1440-1681.2012.05716.x.

Karupiah, G., Xie, Q.W., Buller, R.M.L., Nathan, C., Duarte, C., and MacMicking, J.D. (1993). Inhibition of viral replication by interferon-γ-induced nitric oxide synthase. Science *261*, 1445–1448. https://doi.org/10.1126/science.7690156.

Li, Z., Zhao, Z.J., Zhu, X.Q., Ren, Q.S., Nie, F.F., Gao, J.M., Gao, X.J., Yang, T.B., Zhou, W.L., Shen, J.L., et al. (2012). Differences in *iNOS* and arginase expression and activity in the macrophages of rats are responsible for the resistance against *T. gondii* infection. PLoS ONE *7*, e35834. https://doi.org/10.1371/journal.pone.0035834.

Liu, M.X., Jin, L., Sun, S.J., Liu, P., Feng, X., Cheng, Z.L., Liu, W.R., Guan, K.L., Shi, Y.H., Yuan, H.X., and Xiong, Y. (2018). Metabolic reprogramming by PCK1 promotes TCA cataplerosis, oxidative stress and apoptosis in liver cancer cells and suppresses hepatocellular carcinoma. Oncogene *37*, 1637–1653. https://doi.org/10.1038/s41388-017-0070-6.

Loughran, P.A., Stolz, D.B., Vodovotz, Y., Watkins, S.C., Simmons, R.L., and Billiar, T.R. (2005). Monomeric inducible nitric oxide synthase localizes to peroxisomes in hepatocytes. Proc. Natl. Acad. Sci. U S A *102*, 13837–13842. https://doi.org/10.1073/pnas.0503926102.

Martens, S., Parvanova, I., Zerrahn, J., Griffiths, G., Schell, G., Reichmann, G., and Howard, J.C. (2005). Disruption of *Toxoplasma gondii* parasitophorous vacuoles by the mouse p47-resistance GTPases. PLoS Pathog. *1*, 0187–0201. https://doi.org/10.1371/journal.ppat.0010024.

Masters, B.S., McMillan, K., Sheta, E.A., Nishimura, J.S., Roman, L.J., and Martasek, P. (1996). Neuronal nitric oxide synthase, a modular enzyme formed by convergent evolution: structure studies of a cysteine thiolate-liganded heme protein that hydroxylates L-arginine to produce NO· as a cellular signal. FASEB J. : official Publ. Fed. Am. Societies Exp. Biol. *10*, 552–558. https://doi.org/10.1096/fasebj.10.5.8621055.

Miller, R., Wen, X., Dunford, B., Wang, X., and Suzuki, Y. (2006). Cytokine production of $CD8^+$ immune T cells but not of $CD4^+$ T cells from *Toxoplasma gondii*-infected mice is polarized to a type 1 response following stimulation with tachyzoite-infected macrophages. J. Interferon Cytokine Res. *26*, 787–792. https://doi.org/10.1089/jir.2006.26.787.

Molestina, R.E., and Sinai, A.P. (2005). Detection of a novel parasite kinase activity at the *Toxoplasma gondii* parasitophorous vacuole membrane capable of phosphorylating host IκBα. Cell Microbiol. *7*, 351–362. https://doi.org/10.1111/j.1462-5822.2004.00463.x.

Murray, H.W., Rubin, B.Y., Carriero, S.M., Harris, A.M., and Jaffee, E.A. (1985). Human mononuclear phagocyte antiprotozoal mechanisms: oxygen-dependent vs oxygen-independent activity against intracellular *Toxoplasma gondii*. J. Immunol. *134*, 1982–1988. https://doi.org/10.0000/PMID2981929.

Nathan, C., and Shiloh, M.U. (2000). Reactive oxygen and nitrogen intermediates in the relationship between mammalian hosts and microbial pathogens. Proc. Natl. Acad. Sci. *97*, 8841–8848. https://doi.org/10.1073/pnas.97.16.8841.

Nathan, C., and Xie, Q.wen (1994). Nitric oxide synthases: roles, tolls, and controls. Cell *78*, 915–918. https://doi.org/10.1016/0092-8674(94)90266-6.

Nathan, C.F., and Hibbs, J.B. (1991). Role of nitric oxide synthesis in macrophage antimicrobial activity. Curr. Opin. Immunol. *3*, 65–70. https://doi.org/10.1016/0952-7915(91)90079-G.

Pfannes, S.D.C., Bessler, W.G., Hoffmann, P., Müller, B., and Körner, S. (2001). Induction of soluble antitumoral mediators by synthetic analogues of bacterial lipoprotein in bone marrow-derived macrophages from LPS-responder and -nonresponder mice. J. Leukoc. Biol. *69*, 590–597. https://doi.org/10.1189/jlb.69.4.590.

Scharton-Kersten, T.M., Yap, G., Magram, J., and Sher, A. (1997). Inducible nitric oxide is essential for host control of persistent but not acute infection with the intracellular pathogen *Toxoplasma gondii*. J. Exp. Med. *185*, 1261–1273. https://doi.org/10.1084/jem.185.7.1261.

Schlüter, D., Deckert-Schlüter, M., Lorenz, E., Meyer, T., Röllinghoff, M., and Bogdan, C. (1999). Inhibition of inducible nitric oxide synthase exacerbates chronic cerebral toxoplasmosis in Toxoplasma gondii-susceptible C57BL/6 mice but does not reactivate the latent disease in *T. gondii*-resistant BALB/c mice. J. Immunol. (Baltimore, Md.: 1950) *162*, 3512–3518. https://doi.org/10.1109/TPEL.2003.823249.

Schneider, C.A., Rasband, W.S., and Eliceiri, K.W. (2012). NIH Image to ImageJ: 25 years of image analysis. Nat. Methods. https://doi.org/10.1038/nmeth.2089.

Shen, B., Brown, K.M., Lee, T.D., and David Sibley, L. (2014). Efficient gene disruption in diverse strains of *Toxoplasma gondii* using CRISPR/CAS9. mBio *5*. 01114–14. https://doi.org/10.1128/mBio.01114-14.

Shen, B., Brown, K., Long, S., and Sibley, L.D. (2017a). Development of CRISPR/Cas9 for efficient genome editing in *Toxoplasma gondii*. In Methods in Molecular Biology, A. Reeves, ed. (Springer New York), pp. 79–103. https://doi.org/10.1007/978-1-4939-6472-7_6.

Shen, J., Lai, D.-H., Wilson, R.A., Chen, Y.-F., Wang, L.-F., Yu, Z.-L., Li, M.-Y., He, P., Hide, G., Sun, X., et al. (2017b). Nitric oxide blocks the development of the human parasite Schistosoma japonicum. Proc. Natl. Acad. Sci. *114*, 10214–10219. https://doi.org/10.1073/pnas.1708578114.

Shen, Y., Liu, W.-W., Zhang, X., Shi, J.-G., Jiang, S., Zheng, L., Qin, Y., Liu, B., and Shi, J.-H. (2020). TRAF3 promotes ROS production and pyroptosis by targeting ULK1 ubiquitination in macrophages. FASEB J. 1–16. https://doi.org/10.1096/fj.201903073R.

Sinai, A.P., and Joiner, K.A. (1997). Safe HAVEN: the cell biology of nonfusogenic pathogen vacuoles. Annu. Rev. Microbiol. *51*, 415–462. https://doi.org/10.1146/annurev.micro.51.1.415.

Skulachev, V.P. (1999). Mitochondrial physiology and pathology; concepts of programmed death of organelles, cells and organisms. Mol. Aspects Med. *20*, 139–184. https://doi.org/10.1016/S0098-2997(99)00008-4.

Stolz, D.B., Zamora, R., Vodovotz, Y., Loughran, P.A., Billiar, T.R., Kim, Y.M., Simmons, R.L., and Watkins, S.C. (2002). Peroxisomal localization of inducible nitric oxide synthase in hepatocytes. Hepatology *36*, 81–93. https://doi.org/10.1053/jhep.2002.33716.

Suss-Toby, E., Zimmerberg, J., and Ward, G.E. (1996). Toxoplasma invasion: the parasitophorous vacuole is formed from host cell plasma membrane and pinches off via a fission pore. Proc. Natl. Acad. Sci. United States America *93*, 8413–8418. https://doi.org/10.1073/pnas.93.16.8413.

Wang, X., Liu, Q., Ihsan, A., Huang, L., Dai, M., Hao, H., Cheng, G., Liu, Z., Wang, Y., and Yuan, Z. (2012). JAK/STAT pathway plays a critical role in the proinflammatory gene expression and apoptosis of RAW264.7 cells induced by trichothecenes as don and T-2 toxin. Toxicol. Sci. *127*, 412–424. https://doi.org/10.1093/toxsci/kfs106.

Wang, Y., Cirelli, K.M., Barros, P.D.C., Sangaré, L.O., Butty, V., Hassan, M.A., Pesavento, P., Mete, A., and Saeij, J.P.J. (2019a). Three *Toxoplasma gondii* dense granule proteins are required for induction of Lewis rat macrophage pyroptosis. mBio *10*. e02388–18. https://doi.org/10.1128/mbio.02388-18.

Wang, Y., Shi, P., Chen, Q., Huang, Z., Zou, D., Zhang, J., Gao, X., and Lin, Z. (2019b). Mitochondrial ROS promote macrophage pyroptosis by inducing GSDMD oxidation. J. Mol. Cell Biol. *11*, 1069–1082. https://doi.org/10.1093/jmcb/mjz020.

Werk, R. (1985). How does *Toxoplasma gondii* enter host cells? Rev. Infect. Dis. *7*, 449–457. https://doi.org/10.1093/clinids/7.4.449.

Witola, W.H., Kim, C.Y., and Zhang, X. (2017). Inherent oxidative stress in the Lewis rat is associated with resistance to toxoplasmosis. Infect. Immun. *85*, 1–14. https://doi.org/10.1128/IAI.00289-17.

Xia, X., Wang, X., Zheng, Y., Jiang, J., and Hu, J. (2019). What role does pyroptosis play in microbial infection? J. Cell Physiol. *234*, 7885–7892. https://doi.org/10.1002/jcp.27909.

Yang, C.-S., Yuk, J.-M., Lee, Y.-H., and Jo, E.-K. (2016). *Toxoplasma gondii* GRA7-Induced TRAF6 activation contributes to host protective immunity. Infect. Immun. *84*, 339–350. https://doi.org/10.1128/IAI.00734-15.

Yarovinsky, F. (2014). Innate immunity to *Toxoplasma gondii* infection. Nat. Rev. Immunol. *14*, 109–121. https://doi.org/10.1038/nri3598.

Zeevalk, G.D., Manzino, L., Sonsalla, P.K., and Bernard, L.P. (2007). Characterization of intracellular elevation of glutathione (GSH) with glutathione monoethyl ester and GSH in brain and neuronal cultures: relevance to Parkinson's disease. Exp. Neurol. *203*, 512–520. https://doi.org/10.1016/j.expneurol.2006.09.004.

Zenner, L., Darcy, F., Cesbron-Delauw, M.F., and Capron, A. (1993). Rat model of congenital toxoplasmosis: rate of transmission of three *Toxoplasma gondii* strains to fetuses and protective effect of a chronic infection. Infect. Immun. *61*, 360–363. https://doi.org/10.1128/iai.61.1.360-363.1993.

Zhang, J., Wang, X., Vikash, V., Ye, Q., Wu, D., Liu, Y., and Dong, W. (2016). ROS and ROS-mediated cellular signaling. Oxidative Med. Cell Longevity *2016*, 1–18. https://doi.org/10.1155/2016/4350965.

Zhao, Z.J., Zhang, J., Wei, J., Li, Z., Wang, T., Yi, S.Q., Shen, J.L., Yang, T.B., Hide, G., and Lun, Z.R. (2013). Lower expression of inducible nitric oxide synthase and higher expression of arginase in rat alveolar macrophages are linked to their susceptibility to *Toxoplasma gondii* infection. PLoS ONE *8*, e63650. https://doi.org/10.1371/journal.pone.0063650.

STAR★METHODS

KEY RESOURCES TABLE

REAGENT or RESOURCE	SOURCE	IDENTIFIER
Antibodies		
Anti-SOD2 antibody produced in goat	Sigma-Aldrich	Cat#SAB2501676; RRID: AB_2893357 Lot#10972P1
Anti-β-tubulin mouse monoclonal antibody	TransGen	Cat#HC101; RRID: AB_2893358; Lot#L20817
Rabbit anti-rat caspase-1 antibody	Abcam	Cat#ab179515; RRID: AB_2884954; Lot#GR3232708
Rabbit anti-rat caspase-3 antibody	Abcam	Cat#ab179517; RRID: AB_2893359; Lot#GR3271024-1
Rabbit anti-rat IL-1β antibody	Abcam	Cat#ab9787; RRID: AB_308787; Lot#GR161754-57
Rabbit anti-rat IL-18 antibody	Abcam	Cat#ab191860; RRID: AB_2750951; Lot#GR3243446-9
Anti-GAPDH mouse monoclonal antibody	TransGen	Cat#HC301; RRID: AB_2629434; Lot#M10814
HRP-labeled Goat Anti-Rabbit IgG (H+L)	Beyotime	Cat#A0208; RRID: AB_2892644; Lot#01151818022
Rabbit anti-goat IgG HRP-conjugated antibody	Gentex	Cat# GTX228416-01; RRID: AB_2887582; Lot#41715
Goat anti-mouse IgG (H+L) secondary antibody, HRP	Invitrogen	Cat#31430; RRID:AB_228307; Lot#UB278606
Toxoplasma gondii SAG1 monoclonal antibody	Invitrogen	Cat#MA5-18268; RRID:AB_2539642; Lot#TJ2659778
Goat anti-mouse IgG (H+L) cross-adsorbed ready probes™ secondary antibody, alexa flour 594	Invitrogen	Cat#R37121; RRID: AB_2556549; Lot#2014703
Chemicals, peptides, and recombinant proteins		
Lipopolysaccharide	Sigma-Aldrich	Cas: SMB00610
Interferon-gamma	Sigma-Aldrich	Cas: I3275
Sodium nitroprusside	Sigma-Aldrich	Cas: 13755-38-9
Mn(III) tetrakis (4-benzoic acid) porphyrin	Merck	Cas: 55266-18-7
2′,7′-dichlorofluorescin diacetate	Beyotime	S0033M
VX765	Meilunbio	JYY-S81449-5mg; Cas: 273404-37-8
MCC950	MedchemExpress	Cas: HY-12815A
Critical commercial assays		
Nitric oxide content assays kit	Beyotime	S0023
Total Glutathione Assay Kit	Beyotime	S0052
Hoechst 3342 and Propidium Iodide staining Kit	Beyotime	C1056
Annexin V-FITC and Propidium Iodide staining Kit	Beyotime	C1062M
Deposited data		
Raw and analyzed data	This paper	SRA: PRJNA642722
Experimental models: Cell lines		
Neonates rat muscle fibroblast	This paper	
L929	Procell life Science&technology Co,.Ltd	Cat#CL-0137

(*Continued on next page*)

Continued

REAGENT or RESOURCE	SOURCE	IDENTIFIER
Experimental models: organisms/strains		
iNOS knock out Sprague Dawley rat	Shen et al., 2017b	N/A
GRA43 knockout *T. gondii* RH strain	This paper	N/A
ROP18 Knockout *T. gondii* RH strain	Du et al., 2014	N/A
Oligonucleotides		
Primer for construct plasmids and Diagnostic PCRs, see Table S1	This paper	N/A
Recombinant DNA		
pUPRT::DHFR-D	Shen et al., 2014	N/A
pSAG1-Cas9-sgUPRT	Shen et al., 2014	N/A
pGRA43::DHFR	This paper	N/A
pSAG1-Cas9-sgGRA43	This paper	N/A
Software and algorithms		
ImageJ	Schneider et al., 2012	https://imagej.nih.gov/ij/

RESOURCE AVAILABILITY

Lead contact

- Further information and requests should be directed to and will be fulfilled by the corresponding author, Zhao-Rong Lun (lsslzr@mail.sysu.edu.cn).

Materials availability

- This study did not generate new unique reagents.

Date and code availability

- The transcriptome sequence data has been deposited at NCBI and are publicly available as of the date of publication. Accession number is listed in the key resources table. Original western blot images and microscopy data reported in this paper will be shared by the lead contact upon request.
- This paper does not report any original code.
- Any additional information required to reanalyze the data reported in this paper is available from the lead contact upon request.

EXPERIMENTAL MODEL AND SUBJECT DETAILS

This work was conducted in accordance with protocols approved by the Laboratory Animal Use and Care Committee of Sun Yat-Sen University under the license no. 31772445. Sprague Dawley (SD) rats and Swiss Webster mice were purchased from the Laboratory Animal Center of Sun Yat-sen University, Lewis (LEW) rats were purchased from Vital River Laboratories (Beijing, China), while the source of *iNOS*$^{-/-}$ rats (SD background) was described previously (Shen et al., 2017b). All rats were 4–5 weeks old and weighed 90 $\pm$ 20 g, while all Swiss Webster mice weighed 25–30 g. All animals were allowed free access to water and food under specific pathogen-free conditions. *T. gondii* RH/GFP and PLK/RED strains were provided by Prof. Xue-Nan Xuan, Obihiro University of Agriculture and Veterinary medicine. *T. gondii* RH-Δ*rop18* strain was provided by Jian-Du, Anhui Medical University. RH and PLK strains of *T. gondii* were maintained in human foreskin fibroblasts (HFF), with DMEM supplemented with 10% fetal bovine serum (FBS), 100 μg/ml gentamicin, and 10 mM glutamine at 37°C, 5% CO_2, after thawing from the liquid nitrogen. Tgctsd1 was maintained in mice. In general, tachyzoites were harvested from the peritoneal cavity of infected Swiss Webster mice by inoculation of ice-cold PBS or from the cultures. Rat muscle fibroblast cells split from neonates' rat leg, cultured in plates in an incubator with RPMI-1640 supplemented with 10% FBS, 100 μg/ml gentamicin, and 10 mM glutamine at 37°C, 5% CO_2. Rat PMs were isolated from adult rats peritoneal and incubated in RPMI-1640 supplemented with 10% FBS, 100 μg/ml gentamicin, and 10 mM

glutamine at 37°C, 5% CO_2. Bone marrow precursor cells were isolated from donor rats and differentiated into macrophages as described (Hoffmann et al., 1989; Pfannes et al., 2001). To generate *T. gondii* RH-*Δgra43* strain, GRA43 locus-specific CRISPR plasmid, pSAG1-Cas9-sg*UPRT* was replaced by a *UPRT* targeting guide RNA (gRNA) with a GRA43 gRNA using site-directed mutagenesis as described (Shen et al., 2014, 2017a).

METHOD DETAILS

Animals and parasites

Sprague Dawley (SD) rats and Swiss Webster mice were purchased from the Laboratory Animal Center of Sun Yat-sen University, Lewis (LEW) rats were purchased from Vital River Laboratories (Beijing, China), while the source of *iNOS*$^{-/-}$ rats (SD background) was described previously (Shen et al., 2017b). All rats were 4–5 weeks old and weighed 90 ± 20 g, while all Swiss Webster mice weighed 25–30 g. All animals were allowed free access to water and food under specific pathogen-free conditions.

In order to clarify whether different strains of *Toxoplasma gondii* showed infection profile differences in WT and *iNOS*$^{-/-}$-SD rats, *T. gondii* I strain RH/GFP, type II strain PLK/RED or PRU and a Chinese strain Tgctsd1 (Chinese III) were used (Gao et al., 2017). RH and PLK strains of *T. gondii* were maintained in human foreskin fibroblasts (HFF), with DMEM supplemented with 10% fetal bovine serum (FBS), 100 μg/ml gentamicin, and 10 mM glutamine at 37°C, 5% CO_2, after thawing from the liquid nitrogen. Tgctsd1 was maintained in mice. In general, tachyzoites were harvested from the peritoneal cavity of infected Swiss Webster mice by inoculation of ice-cold PBS or from the cultures.

Chemicals

Key chemicals used in our experiments are listed as follows: Lipopolysaccharide (LPS) (Sigma, USA), interferon-gamma (IFN-γ) (Sigma, USA), sodium nitroprusside (SNP) (Sigma, USA), Mn(III) tetrakis (4-benzoic acid) porphyrin (MnTBAP) (Merck, USA), VX765 (Meilunbio, China), MCC950 (MedChemExpress, USA).

Antibodies

Anti-SOD2 antibody produced in goat (1:1000; Sigma, USA), anti-β-tubulin mouse monoclonal antibody (1:1000; TransGen Biotech, China), rabbit anti-rat caspase-1 antibody (1:1000; Abcam, England), rabbit anti-rat caspase-3 antibody (1:1000; Abcam, England), rabbit anti-rat IL-1β antibody (1:1000; Abcam, England), rabbit anti-rat IL-18 antibody (1:1000; Abcam, England), anti-GAPDH mouse monoclonal antibody (1:1000; TransGen Biotech, China). Secondary antibody: HRP-labeled goat anti-rabbit IgG (H + L) (1:1000; Beyotime, China), goat anti-mouse IgG (H + L) secondary antibody, HRP (Invitrogen, USA), rabbit anti-goat IgG HRP-conjugated antibody (1:1000; Gentex, USA), *Toxoplasma gondii* SAG1 monoclonal antibody (1:20; Invitrogen, USA), goat anti-mouse IgG (H + L) cross-adsorbed ReadyProbes™ secondary antibody, and alexa fluor 594 (1:1000; Invitrogen, USA).

In vivo parasite infection and bioassay

To determine the survival ratio of SD rats infected with *T. gondii* tachyzoites, each SD rat was intraperitoneally (i.p.) inoculated with 10^7 tachyzoites (strains of RH/GFP, PLK/RED or Tgctsd1) in 500 μL PBS. The sera were collected from the group of SD rats infected with *T. gondii* as above and the control group of rats were injected only with 500 μL PBS. Sera were collected from infected rats at 3, 6 and 9 dpi. IFN-γ concentration was determined using the rat IFN-γ ELISA kit (ExCell Biotech, China).

Furthermore, to test cyst forming ability, *iNOS*$^{-/-}$-SD rats were i.p. infected with 10^6 tachyzoites of a cyst forming strain of *T. gondii* Tgctsd1 as described previously (Gao et al., 2017), while Prugniaud (PRU) strain was used as a reference. *T. gondii* cyst numbers were counted in brain homogenates from the infected SD rats at 60 dpi.

For bioassay, rats infected with *T. gondii* RH strain were sacrificed at 3, 6, 10, 20 and 30 dpi, while rats infected with the PLK/RED and Tgctsd1 strains were killed at 60 dpi. Heart, liver, spleen, lung, kidney and brain (3 and 6 dpi rats were not detected) were collected from each sacrificed rat and 0.5 g tissue from each organ was homogenized in 1 mL PBS (pH = 7.4) and was i.p. inoculated into a swiss mouse. The mice were monitored in a daily manner until they were sacrificed 30 days later.

Histological analysis of brain tissue sections

To monitor the brain cysts in rat, brain tissues were fixed with 4% paraformaldehyde solution for 24h, then dehydrated, embedded in paraffin and sectioned into slices of 4–6 μm. Slices were hydrated in xylene and a descending sequence of ethanol, following hematoxylin-eosin (H&E) stain.

Preparation of primary fibroblasts, peritoneal macrophages and bone marrow derived macrophages

Rat neonates were sterilized with 75% alcohol for 5 min and sacrificed. Muscle tissues from legs were collected, snipped into pieces and digested with 0.05% (w/v) trypsin/0.53 mM EDTA at 37°C for 5 min until termination with 10% FBS in RPMI-1640. Muscle cells were passed through a filter with 70.0-μm pore (Biologix, USA) to discard debris and were cultured in the plates in an incubator with 5% CO_2 at 37°C for 4 hours. Non-adherent cells were washed away and the remaining cells, termed SD rat neonatal muscle fibroblast cells (NMFCs), were continuously cultured for further experiments. Rat NMFCs were also subcultured and stored in liquid nitrogen for later use.

For the macrophage isolation, adult rats were sterilized and sacrificed as above. They were then i.p. inoculated with 15 ml ice cold PBS. Peritoneal fluid was collected, centrifuged and washed with FBS-free RPMI-1640 medium, and cells were transferred to a 24-well (5×10^5 per well) plate. Non-adherent cells were washed away after 1h incubation and the remaining cells, the rat peritoneal macrophages (PMs) were used for further experiments.

Bone marrow precursor cells were isolated from donor rats and differentiated into macrophages as described (Hoffmann et al., 1989; Pfannes et al., 2001). Briefly, bone marrow cells were washed out with RPMI-1640 from the femurs and tibias isolated from SD rats aged 6 weeks. Macrophages were obtained by cultivation of the precursor cells for 5–7 days in a differentiation medium of Dulbecco's modified Eagle's medium (DMEM) supplemented with 10% L-cell-conditioned medium, 10% heat-inactivated FBS, 1% penicillin and streptomycin (Invitrogen, USA) at 37°C and 5% CO_2.

Treatments of rat cells and parasite infection

Rat NMFCs and rat PMs were pre-treated with the designated factor(s) of either 100 ng/ml lipopolysaccharide (LPS) or/and 100 ng/ml interferon-gamma (IFN-γ) for 12 hours, or with 25 μM sodium nitroprusside (SNP) for 12h, or with 50 μM VX765 or 10 μM MCC950 for 2 hours.

All *T. gondii* tachyzoites were collected and purified with a 5.0-μm pore filter (Millipore, USA). The filtrate was then centrifuged at 1000×g for 10 min at 4°C, resuspended in RPMI-1640 medium (GIBCO, USA) supplied with 10% FBS. For *in vitro* experiments, tachyzoites were added to the cells in RPMI-1640 medium at a multiplicity of infection (MOI) of 2 and were allowed to invade for 1 hour at 37°C in 5% CO_2. The free tachyzoites were washed away with PBS and the complete RPMI-1640 medium was pretreated with designated factor(s). This was recorded as 0 hpi (hours post infection).

Determination of nitric oxide (NO), reactive oxygen species (ROS) and glutathione (GSH)

To test the NO content, rat PMs were treated with LPS or/and IFN-γ as described above. Media from the preparations with or without *T. gondii* were collected at 24 hpi and centrifuged. Supernatants were used to determine NO content as previously described (Li et al., 2012).

ROS generated in RPMs was determined with 2′,7′-dichlorofluorescin diacetate (DCFH-DA) (Beyotime, China) using flow cytometry or confocal microscopy as described (Liu et al., 2018). For flow cytometry, rats were i.p. injected with 10^7 tachyzoites, and RPMs were collected 1h later. The harvested cells were then incubated in FBS and phenol red free RPIM-1640 with 10 μM DCFH-DA (Beyotime, China) at 37°C for 30 min. Subsequently, cells were washed with ice cold PBS three times and analyzed using a FACSCanto II flow cytometer (BD Biosciences, USA) at 495 nm excitation and 529 nm emission.

For confocal microscope analysis, the naïve rat PMs were collected from uninfected rats, grown on the confocal dishes for adherence for 1h. After washing, PMs were infected with *T. gondii* for 1h and non-invaded parasites were washed away. After another hour of incubation, the DCFH-DA probe was added

as described above. Samples were then washed with ice cold PBS three times and imaged under the LSM880 confocal microscope (Zeiss, Germany).

To test the GSH content, RPMs were obtained from infected rats 3 hours after inoculation as mentioned above, cellular lysis was conducted in ice-cold buffer and the protocol was followed as reported (Fan et al., 2012). The GSH content in the cell lysis was measured following the manufacturer's instructions for the Total Glutathione Assay Kit (Beyotime, China).

Sample preparation for transmission electron microscopy

Rat PMs were isolated from infected and noninfected rats 3 hpi with 10^7 *T. gondii* PLK/RED strain tachyzoites as mentioned above, and were fixed, dehydrated, and embedded. Ultrathin sections were observed under the JEM1400 electron microscope (JEOL, Japan).

Western-blotting

Rat PMs were harvested as described above and were lysed by rapid repeated freezing in liquid nitrogen and thawing in a 37°C water bath (three times). Protein concentrations were determined using the BCA protein assay kit (Beyotime, China). Samples were denatured, resolved on 15% SDS-PAGE gels, transferred onto polyvinylidene fluoride (PVDF) membranes (Pall, USA), blocked with 5% nonfat milk in TBS (Tris-buffered saline) and subsequently probed with designated 1st and 2nd antibodies. Signals were detected using a *Tanon*™ High-sig ECL Western Blotting Detection Kit (Tanon, China) using Thomas' methods (Hnasko and Hnasko, 2015).

Determination of the effect of GSH and MnTBAP on the growth of *T. gondii* in SD and LEW RPMs

Fresh rat PMs isolated from SD and LEW rats were transferred at a density of 5×10^5 per well onto the 24-well plates with 1 ml of supplemented RPMI-1640 medium mentioned as above. Triplicate wells were treated with the ROS scavenger Mn(III) tetrakis (4-benzoic acid) porphyrin (MnTBAP) (Gauuan et al., 2002) (200 μM, Merck, USA) and antioxidants of GSH (Zeevalk et al., 2007) (2 mM, Beyotime, China), incubated for 6 h, and then were infected with tachyzoites of *T. gondii* RH/GFP strain at a MOI of 2, followed by incubation at 37°C with 5% CO_2 and humidity. After incubation at 12, 24 and 48h, the cultures were analyzed by fluorescence microscopy using the fluorescein isothiocyanate (FITC) channel to measure the parasite GFP fluorescence. After 24h time points of analysis, the medium was completely aspirated from each well and replaced with an equivalent volume (1 mL) of fresh medium containing fresh GSH or MnTBAP at the respective final concentration. To determine the *T. gondii* infection ratio in the *iNOS*$^{-/-}$-SD, WT-SD and LEW rat PMs treated with or without GSH and MnTBAP, microscopic images of fields of view were captured for infection analysis. Fluorescent quantification was done using ImageJ software (version 1.37).

Cell viability assay

To assess cell viability after infection with *T. gondii* in the presence of the ROS burst, Hoechst 33342 and Propidium Iodide (PI) staining assays were performed (Chen et al., 2015). PMs were freshly isolated from *iNOS*$^{-/-}$-SD, WT-SD and LEW rat strains. Cells were transferred into 24-well plates as described above with RPMI-1640 medium complemented with FBS (10%). Tachyzoites of the *T. gondii* RH/GFP strain were infected at a MOI of 2. PMs with or without *T. gondii* infection were incubated for 4 h at 37°C with 5% CO_2 and humidity. After 4h, the cells were washed twice with PBS and 1 mL of RPMI-1640 with 5 μL propidium iodide (PI) and 5 μL Hoechst (Beyotime, China) was added. Cells were incubated at 4°C for 20 min, then washed twice with PBS and pooled in 1 mL of PBS. Images were taken using a ZEISS microscope and the stained cells were counted. Confocal imaging was performed using a ZEISS 880 Confocal laser microscope. WT-SD rat PMs as the positive control were incubated with apoptosis inducers (Beyotime, China) at a dilution of 1:1000 for 4 h.

For cell death verification, fresh PMs isolated from *iNOS*$^{-/-}$-SD, WT-SD and LEW rat were transferred to flow tubes (1×10^6 per tube) with 2 mL of complete RPIM-1640 medium at 37°C with 5% CO_2 and humidity. Rat PMs with or without *T. gondii* infection at a MOI of 1 were incubated for 4h at 37°C with 5% CO_2 and humidity. Positive control WT-SD rat PMs were incubated as described above. PMs were then collected by centrifugation and assessed with Annexin V-FITC and PI staining (Beyotime, China) for 10 min as described

(Wang et al., 2012). Data acquisition was performed by flow cytometry on a MoFlo-XDP (Beckman Coulter, USA) and analysis was conducted with the FlowJo software (v10.3).

GRA43 knock-out and cell infection

To generate the GRA43 locus-specific CRISPR plasmid, pSAG1-Cas9-sg*UPRT* was replaced by a *UPRT* targeting guide RNA (gRNA) with a GRA43 gRNA using site-directed mutagenesis as described (Shen et al., 2014, 2017a). To construct a homologous template for the GRA43 knockout, the 5′ and-3′ homology arms of *GRA43* gene were amplified by PCR from the RH strain genome and the selection marker *DHFR* was amplified from pUPRT::DHFR-D. The 5′ and-3′ homology arms, as well as *DHFR*, were cloned into pUC19 using the ClonExpress II One Step Cloning Kit (Vazyme Biotech, Nanjing, China) (Figure S8). All primers used to construct plasmids are listed in Table S2. All plasmids were confirmed by DNA sequencing. To generate the GRA43 knockout RH strain (RH-Δ*gra43*), an homology template was amplified from plasmid pGRA43::DHFR and co-transfected with pSAG1-Cas9-sgGRA43 into 10^7 RH tachyzoites which were suspended in 100 μL Cytomix using an Amaxa electroporation system and the X-001 program. Transfectants were selected with 2 μM pyrimethamine (Sigma Aldrich, USA), cloned by limiting dilution in 96-well plates and verified by diagnostic PCRs (primers listed in Table S2) (Figure S8).

Immunofluorescence assays (IFA)

To assess the *ROP18* or *GRA43* knock-out *T. gondii* infection ratio, the infected RPMs were subjected to immunofluorescence assays as reported (Du et al., 2014). Briefly, PMs cultured on the coverslips in 24-well plates were infected with RH, RH-*Δrop18* and RH-Δ*gra43* tachyzoites at a MOI of 2 respectively. At 24 or 48 hours after infection, cells were washed with PBS three times and fixed in 4% paraformaldehyde (PFA) for 15 min, then were quenched and permeabilized with 0.2% Triton X-100 and 0.2 M glycine in PBS for 20 min, and then blocking in 3% bovine serum albumin (BSA) in PBS for 30 min. A subsequent incubation with mouse monoclonal anti-SAG1 primary antibody (Invitrogen) was applied for 3 h at 37°C, followed by rabbit anti-mouse Alexa Fluor 594 (Thermo Fisher) for 1 h at 37°C. After washed with PBS three times, cells were stained with 4,6-Diamidino-2-phenylindole (DAPI) and examined under a microscope (Leica). Images were recorded for further use.

Determination of ROS in RPMs infected with the *T. gondii* RH-Δ*gra43*

Rat PMs were collected and incubated in a 24-well plate as mentioned before. Cells were infected with *T. gondii* RH or RH-Δ*gra43* and non-infected cells were used as control. The DCFH-DA probe was added to the cells at 1 hpi and 3 hpi respectively, then they were incubated for 30 min and washed as mentioned above (Liu et al., 2018). Results were observed and recorded under a Zeiss microscope and were analyzed by ImageJ (Version 1.52a).

RNA extraction, library preparation and RNA sequencing

Rats were i.p. injected with 10^7 tachyzoites or equal volume of 1×PBS. After 3 h inoculated, 1×10^7 peritoneal cells were used for total RNA extraction for each rat. Total RNA of each sample from individual animals was extracted using TRIzol Reagent (Invitrogen). RNA samples were quantified and qualified by 2100 Bioanalyzer (Agilent Technologies, Palo Alto, CA, USA), NanoDrop (Thermo Fisher Scientific Inc.) and 1% agrose gel. 1 μg total RNA with RIN value above 7 was used for following library preparation. RNA library preparation and sequencing were performed at the GENEWIZ Inc High Throughput Sequencing according to the manufacturer's protocol (NEBNext® UltraTM RNA Library Prep Kit for Illumina®). Libraries with different indices were multiplexed and loaded on an Illumina HiSeq instrument according to manufacturer's instructions (Illumina, San Diego, CA, USA). Sequencing was carried out using a 2x150bp paired-end (PE) configuration; image analysis and base calling were conducted by the HiSeq Control Software (HCS) + OLB + GAPipeline-1.6 (Illumina) on the HiSeq instrument. The sequences were processed and analyzed by GENEWIZ Inc. All raw data were up-loaded to NCBI and the bioproject number is PRJNA642722.

QUANTIFICATION AND STATISTICAL ANALYSIS

Statistical analysis was performed and illustrated using GraphPad Prism software (version 8.0). The data are given as the means ± standard deviation or means ± standard error of mean and are representative from at least three independent experiments. Statistical significance was accepted at $p < 0.05$, using the Student's unpaired t test or and performed two-tailed χ2-test (Fisher's exact test).